



Review

Recent advances in carbon nanostructures prepared from carbon dioxide for high-performance supercapacitors

Chen Li^{a,b}, Xiong Zhang^{a,b,d,*}, Kai Wang^{a,b,d}, Fangyuan Su^{c,d}, Cheng-Meng Chen^{c,d}, Fangyan Liu^d, Zhong-Shuai Wu^d, Yanwei Ma^{a,b,*}^a Institute of Electrical Engineering, Chinese Academy of Sciences, Beijing 100190, China^b School of Engineering Sciences, University of Chinese Academy of Sciences, Beijing 100049, China^c CAS Key Laboratory of Carbon Materials, Institute of Coal Chemistry, Chinese Academy of Sciences, Taiyuan 030001, Shanxi, China^d Dalian National Laboratory for Clean Energy, Dalian Institute of Chemical Physics, Chinese Academy of Sciences, Dalian 116023, Liaoning, China

ARTICLE INFO

Article history:

Received 8 May 2020

Revised 26 May 2020

Accepted 26 May 2020

Available online 05 June 2020

Keywords:

Carbon materials

Supercapacitors

CO₂ conversion

Nanostructures

ABSTRACT

The burgeoning global economy during the past decades gives rise to the continuous increase in fossil fuels consumption and rapid growth of CO₂ emission, which demands an urgent exploration into green and sustainable devices for energy storage and power management. Supercapacitors based on activated carbon electrodes are promising systems for highly efficient energy harvesting and power supply, but their promotion is hindered by the moderate energy density compared with batteries. Therefore, scalable conversion of CO₂ into novel carbon nanostructures offers a powerful alternative to tackle both issues: mitigating the greenhouse effect caused by redundant atmospheric CO₂ and providing carbon materials with enhanced electrochemical performances. In this tutorial review, the techniques, opportunities and barriers in the design and fabrication of advanced carbon materials using CO₂ as feedstock as well as their impact on the energy-storage performances of supercapacitors are critically examined. In particular, the chemical aspects of various CO₂ conversion reactions are highlighted to establish a detailed understanding for the science and technology involved in the microstructural evolution, surface engineering and porosity control of CO₂-converted carbon nanostructures. Finally, the prospects and challenges associated with the industrialization of CO₂ conversion and their practical application in supercapacitors are also discussed.

© 2020 Science Press and Dalian Institute of Chemical Physics, Chinese Academy of Sciences. Published by ELSEVIER B.V. and Science Press. All rights reserved.

Contents

1. Introduction	354
2. Essential design strategies for carbon-based electrode materials	354
3. Recent progresses in carbon materials prepared from carbon dioxide	356
3.1. Direct metallothermic combustion with CO ₂	356
3.2. High-temperature reduction in CO ₂ flow	358
3.3. Carbonate-assisted conversion of CO ₂	360
3.4. Controllable self-sustaining reaction with CO ₂	363
4. Conclusions and future perspectives	365
Declaration of Competing Interest	366
Acknowledgments	366
References	366

* Corresponding authors at: Institute of Electrical Engineering, Chinese Academy of Sciences, Beijing 100190, China.

E-mail addresses: zhangxiong@mail.iee.ac.cn (X. Zhang), ywma@mail.iee.ac.cn (Y. Ma).



Chen Li completed his B.S. study in polymer materials and engineering at Beijing University of Chemical Technology (BUCT) in 2010, and obtained his Ph.D. degree in electrical engineering from University of Chinese Academy of Sciences (UCAS) in 2017. At the same year, he joined the Institute of Electrical Engineering (IEE), Chinese Academy of Sciences (CAS). His research interests focus on the design and fabrication of advanced carbon-based energy materials for high-performance supercapacitors and lithium-ion capacitors.



Xiong Zhang received his B.S. in applied chemistry from Central South University in 2003, and his Ph.D. in applied chemistry from Beijing University of Chemical Technology in 2008. Then he joined the Institute of Electrical Engineering, Chinese Academy of Sciences. His research interests focus on the synthesis of electrode materials for supercapacitors and the applications of lithium-ion capacitors.



Kai Wang received his B.S. from the Department of Chemistry and Chemical Engineering of Shandong University (2007), and his Ph.D. from National Center for Nanoscience and Technology (NCNST). After a post-doctoral experience in Singapore-MIT Alliance for Research and Technology (SMART), he joined Institute of Electrical Engineering, Chinese Academy of Science in 2014. His current research interests are in the field of electrochemical energy materials and devices, with a focus on hybrid nanomaterials, supercapacitors and solid-state lithium ion batteries.



Fangyuan Su received his Ph.D. in Applied Chemistry (Electrochemistry) from Tianjin University in 2012, and worked as a postdoctor at Tsinghua University in 2012–2014. Then he joined Institute of Coal Chemistry, CAS in 2014, and now works as an associate professor. He has published about 40 research articles. His research focuses on design and simulation of electrochemical energy storage devices including supercapacitor, Li-ion battery and Li-S battery.



Cheng-Meng Chen serves as deputy director of CAS Key Laboratory of Carbon Materials, and principle investigator of Group 709 at Institute of Coal Chemistry, Chinese Academy of Sciences (ICC, CAS). Prof. Chen is committed to the research and development of advanced carbon materials and their applications in energy storage devices. He has been in charge of more than 20 projects, published about 120 papers, held 19 granted patents, published 1 book at Springer, and directed 6 international and national standards. Based on the above achievement, he won the first prize of Natural Science Award of Shanxi Province, and Hou

Debang Youth Award of Chemical Engineering Technology, etc. Prof. Chen was selected as the MIT Technology Review 2017 innovator under 35 in China, and got

the foundation of Outstanding Youth Fund by National Natural Science Foundation of China in 2019.



Fangyan Liu received her Ph.D. from Northeast Forestry University in 2015. She worked as a postdoctor focused on high-energy supercapacitors in Southwest Jiaotong University in 2015–2019, and continued to conduct the postdoctoral research for high-energy energy storage devices in Dalian Institute of Chemical Physics, CAS until now. She has published 15 research articles in *J. Mater. Chem. A*, *Carbon*, *Electrochim. Acta* etc. Her research interests mainly concentrate on 2D materials for high-energy supercapacitors and Li-ion capacitors.



Zhong-Shuai Wu received his Ph.D. from the Institute for Metal Research, CAS in 2011 and worked as a post-doctoral fellow at the Max Planck Institute for Polymer Research in Mainz, Germany from 2011 to 2015. Subsequently, Dr. Wu became a full Professor and Group Leader of 2D Materials & Energy Devices at DICP, CAS and was promoted in 2018 as a DICP Chair Professor. Currently, Prof. Wu's research interests include graphene and 2D materials, surface- and nanoelectrochemistry, microscale electrochemical energy storage devices, supercapacitors, batteries and catalysis. He is a recipient of the National Natural Science Award (2nd class, 2017), the 2018 and 2019 High Cited Researchers (Clarivate Analytics), and the Fellow of the Royal Society of Chemistry. He is an editor of *Applied Surface Science*, Section editor of *Journal of Energy Chemistry*, and editorial board of *Energy Storage Materials*, *Journal of Physics: Energy*, and *Physics*.



Yanwei Ma received his Ph.D. degree from Tsinghua University in 1996 and then worked as a post-doctoral fellow at University of Science and Technology Beijing (USTB). Following research associate positions at Institute for Materials Research, Tohoku University (Sendai, Japan), National Institute for Materials Science (Tsukuba, Japan) and Universite de Rennes 1 (France), he joined the Institute of Electrical Engineering, Chinese Academy of Sciences in 2004 as a full-time professor. He leads a team focused on superconductivity and new energy materials. His research activities are devoted to the development of superconducting wires and nanomaterials for energy storage, and fabrication of graphene-based supercapacitors. He has published more than 300 refereed journal papers, and holds more than 60 international and Chinese innovation patents in the fields. He has given 62 invited talks at international conferences.

1. Introduction

The surging global economy since the advent of 21st century gives rise to rapid consumption of fossil fuels and serious greenhouse problem, which have become major issues in the sustainable development of human society [1–3]. Efficient energy storage plays a key role in building a low-carbon economy to substantially propel the utilization of renewable energy resources [4–7]. As an important energy storage device, supercapacitor has received much attention from both academia and industry. Compared with commercial rechargeable batteries relying on intercalation mechanism in the crystalline structure of electrode materials, supercapacitors can exhibit multiple merits such as high power density, excellent rate performance, long life span and quick charge/discharge, because their charge storage is based on the surface reactions of electrode materials without ion diffusion within the bulk of materials [8–12]. The promising prospect of supercapacitors can be found in compensating energy storage functions of batteries or fuel cells by providing back-up power and preventing power disruptions, which serve as important complementary devices for military purposes, electrical vehicles, smart instruments and portable electronic devices [13–16].

For most of the state-of-the-art commercial supercapacitors, numerous carbon materials with contrasting physical and chemical properties act as typical active materials in electrodes [17–19]. Among them, activated carbon (AC) is widely used as a practical electrode material due to its advantages of high specific surface area, low cost and mature preparation technologies [20–23]. However, supercapacitors based on AC usually present a much lower energy density ($\sim 15\text{--}20\text{ Wh kg}^{-1}$) than lithium-ion batteries (up to $250\text{--}300\text{ Wh kg}^{-1}$) [24–27], which is considered as a great obstacle for its further application in electronic devices requiring high energy and high power simultaneously. To solve this problem, current researches mainly focus on enhancing the energy density of supercapacitors without sacrificing their high power density and long life span. In this scenario, the foremost theme is to seek novel pathways for the fabrication of advanced carbon materials with substantially enhanced energy storage performance. Various carbon nanostructures have been examined in the past decades for application in various energy-related occasions, including AC from numerous precursors [28], carbon nanotube [29,30], carbon nanofiber [31], carbon nanosphere [32], fullerene [33], hard/soft carbon [34–37], carbide-derived carbon [38], porous carbon [39], carbon foam [40] and graphene [41]. Unfortunately, toxic and hazardous chemicals are usually involved for the preparation and chemical/physical modification of carbon materials though various morphological and structural regulation can be achieved [42]. The development of an environment-friendly approach for both safe and practical processing of advanced carbon materials is still a great challenge.

At present, more than 80% of the energy consumed worldwide is derived from non-renewable fossil fuels such as coal, oil and natural gas [43]. The combustion of these fuels inevitably leads to huge emission of CO_2 , a main driver of global climate change and other serious environmental effects [44–46]. Historically, the CO_2 in atmosphere has risen from 278 ppm in the beginning of industrial revolution to more than 400 ppm in 2016. Actually almost 75% of this rise has taken place since 1950. Moreover, the global CO_2 emission has doubled from 1975 to 2015 and is projected to triple by 2040 [47,48]. Although mitigating climate issue is a multifaceted challenge, one of these pillars of any future low-carbon economy will be an increasing dependence on renewable and environmentally friendly pathways to recycle CO_2 into various useful resources. Currently, the utilization and sequestration of CO_2 mainly focuses on using it as an alternative carbon feedstock for

chemicals, fuels and other derivative materials. Among these efforts, catalytic, photocatalytic and electrocatalytic conversion of CO_2 into methane, methanol and hydrocarbon products have made important progresses [49–51]. Encouraged by these achievements, researchers also expect new methodologies to realize direct conversion of CO_2 into materials related with renewable energy storage.

Selective reduction of CO_2 into pure carbon is envisaged as a promising alternative for greenhouse gas recycling; however, the high stability of C=O bond in CO_2 renders it a great difficulty [52]. An early research by Tamaura et al. [53] reported that oxygen deficient ferrites could be used as catalyst to decompose CO_2 into carbon and oxygen. Motiei et al. [54] proved that nested fullerene could be synthesized from supercritical CO_2 . Diamonds could also be prepared from the chemical reaction between CO_2 and metallic Na at $440\text{ }^\circ\text{C}$ and 80 MPa [55]. In the past few years, to further promote CO_2 -derived carbonaceous materials for energy storage, various carbon-based nanostructures, such as graphene [56], graphene oxide [57], carbon nanosheets [58], carbon nanotubes [59,60], carbon nanofiber [61] and porous carbon [62], have been successfully fabricated from CO_2 precursor using strong reducing agents via different preparation technologies, demonstrating CO_2 conversion has become a technologically mature field. In these works, researchers' main aim is to obtain carbon products with high specific surface area, optimized pore size distribution and beneficial functional groups for the enhancement energy storage capacity of supercapacitors. Despite all these achievements in this area, a systematic retrospect on the processing approaches of CO_2 -based nanostructures and their application for energy-related purposes has not been presented so far. It is highly necessary to summarize the latest preparation technologies and offer a panoramic view for carbon materials by CO_2 conversion toward energy storage applications.

In this first review on CO_2 -converted carbon materials, we aim to depict a complete developmental story of various CO_2 utilization methodologies for the microstructural design, surface engineering and porosity control of novel carbon nanostructures along with their recent applications in high-performance supercapacitors. Starting from an introduction to the general design strategies for carbon-based electrodes, different techniques to convert CO_2 into advanced carbon materials are further discussed with special emphasis on their technological shift, product quality control and environmental friendliness. In particular, the detailed processing protocols for CO_2 -based carbon are highlighted to shed light on the important role of microstructure and physiochemical properties on capacitive performances in these carbon materials. This review ends with a brief conclusion to carbon materials manufactured from CO_2 conversion and possible solutions to major challenges for their future application in energy-related fields.

2. Essential design strategies for carbon-based electrode materials

For state-of-the-art carbon-based supercapacitors, the energy storage mechanism originates from the reversible electrostatic accumulation of ions with opposite charges on the interface between porous carbon electrodes and electrolyte, which was depicted by Helmholtz model in 1853 [63]. When the electrode is polarized by applying a voltage, ions with opposite charge in the electrolyte diffuse to the vicinity of carbon electrodes and generate a condensed electrical double layer (EDL) with a thickness of a few nanometers to ensure charge neutrality. The electrode potential decreases as the distance between the ions and the electrode increases (Fig. 1a). This simplified Helmholtz EDL can be regarded as a flat-plate capacitor with the capacitance (C) defined by Eq. (1):

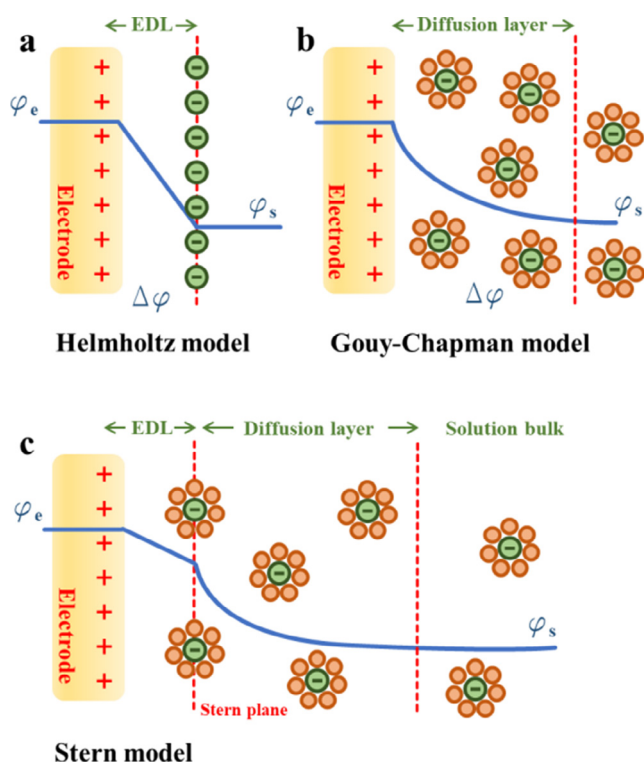


Fig. 1. (a) Helmholtz, (b) Gouy-Chapman, and (c) Stern model of charge storage mechanisms across the interface of electrode and aqueous electrolyte. The potential decreases from φ_e at electrode surface to φ_s at the bulk electrolyte, which can be considered infinite away from the electrode surface.

$$C = \frac{A\varepsilon}{4\pi d} \quad (1)$$

where A is the active surface of the porous electrode; ε is the electrolyte dielectric constant, and d is the effective thickness (Debye length) of EDL [64]. Typically, the very large surface area (up to $3000 \text{ m}^2 \text{ g}^{-1}$) and short Debye length of less than 1 nm for porous carbon electrodes result in a much higher EDL capacitance than flat-plate capacitors [65].

Although Helmholtz model give a direct explanation to the origin of capacitance in carbon electrodes, it simplifies several important factors such as ion diffusion in the electrolyte solution and the static interaction between solvated ions and electrode. In 1910, Gouy and Chapman [66] proposed a diffusion model to depict the exponentially decreasing potential from the electrode surface to the interior of electrolyte solution (Fig. 1b), but this model is not enough to account for highly charged EDL. Later, Stern [67] combined the essentials of Helmholtz and Gouy-Chapman models by introducing the hydrodynamic movement of the ions in the diffusion layer and the accumulation of ions adherent to the electrode surface (Fig. 1c). The total capacitance can be regarded as a Helmholtz layer C_H and a diffuse layer C_D connected in series, which is expressed by Eq. (2):

$$\frac{1}{C} = \frac{1}{C_H} + \frac{1}{C_D} \quad (2)$$

However, since the electrolyte concentration in commercial supercapacitors is usually high ($\sim 1 \text{ mol L}^{-1}$), the diffusion capacitance can be reasonably omitted [68–70]. Therefore, the basic properties of Helmholtz layer determine the charge storage capacity of carbon materials, which are also closely correlated with the surface and porosity structures of electrodes.

The stored energy E in a supercapacitor is directly related with the capacitance and the square of voltage according to Eq. (3):

$$E = \frac{1}{2} CV^2 \quad (3)$$

The maximum power depends on the applied voltage and equivalent series resistance (R_{ESR}), which is given by Eq. (4)

$$P = \frac{V^2}{4R_{\text{ESR}}} \quad (4)$$

R_{ESR} can be considered as the sum of ionic resistance of electrolyte impregnated in the separator, contact resistance between electrodes and current collectors, and intrinsic electrical resistance of electrode bulk [71]. From the above analysis, it can be clearly seen that C , V and R_{ESR} are three important parameters defining the performance of supercapacitor devices, which means great efforts should be devoted to increasing both C and V and reducing R_{ESR} for the simultaneous improvement of energy and power density.

In the viewpoint of material sciences, the primary synthetic target of carbon electrodes is to obtain novel carbon nanostructures with modified interfacial properties between electrode and electrolyte [72]. This requires a careful correlation between electrode microstructure and overall electrochemical behavior. Generally, an ideal carbonaceous electrode should exhibit several key features:

- (1). High accessible surface area. The energy storage capability of carbon electrodes highly relies on the electrical double layer across the interface between electrode and electrolyte. As a result, high surface area can promote sufficient space for charge accumulation and increase the specific capacitance and energy density. During the past years, various nanostructured carbon materials, including 0D quantum dots [73], 1D nanotubes or nanofibers [74,75], 2D nanosheets [76] and 3D foams or aerogels [77–79], have received extensive attention from researchers to shorten the diffusion length of electrolytes and enlarge the exterior surface area in order to obtain a very fast charge/discharge rate and high charge storage. However, materials with extremely high surface area usually present another problem of low tap density. This means a large amount of pores, voids and channels inside these materials, which would trap additional electrolyte as ‘dead mass’ and jeopardize the energy storage of devices [80]. To tackle this paradox, a careful balance between porosity design and morphological control should be considered in fabricating carbon electrodes.
- (2). Designed pore size distribution. A reasonable porosity in electrode materials is also key to influence its wettability and accessibility of surface area to shuttling ions [81]. Micropores (less than 2 nm) can greatly increase the specific surface area of electrodes and contribute to the high charge storage performance, while mesopores in the range of 2 to 50 nm mainly provide interconnected channels for fast ion transportation at high rates [82–84]. On the other hand, macropores (larger than 50 nm) serve as ‘ion reservoir’ to buffer the sharp change of electrolyte concentration during operation at high current density [85]. One risk for macropores is they are prone to absorb extra electrolyte in the pore channels and increase the total weight of devices. Now it has been widely acknowledged that a hierarchical porosity with an optimized proportion of micropores and mesopores is helpful to enhance the ion diffusion behavior and thusly increase the rate capability and power density of electrodes [86].
- (3). Good intra/inter-particle electrical conductivity. A high inter/intra-particle conductivity can ensure swift electron transportation throughout the electrode bulk, minimize internal resistance and promote charge transfer, which are all beneficial for efficient energy storage. For carbon materials, a high percentage of sp^2 -hybridization contributes to the

delocalized electron structure and enhanced conductivity [87,88], which can be realized by high-temperature annealing to remove the insulating oxygen-related functionalities. Reasonable hetero-atom doping can also regulate the electrical conductivity by contributing to the electron density of carbon atoms [89–92]. Another feasible solution is to incorporate conducting agent like carbon black into the electrode or build bridged structure between electrode particles to enhance the inter-particle electron transfer.

- (4). Long-term electrochemical stability. Carbon materials are generally considered electrochemically stable for energy storage because their energy storage mechanism of charge separation at the electrical double layer across the electrode/electrolyte interface introduces no phase change or chemical reaction of electrodes. However, in organic electrolytes and ionic liquids, the trace impurities (ash content, heteroatoms, absorbed H₂O) in carbon electrodes are prone to interact with the solvated ions due to the catalytic decomposition, which will cause irreversible parasitic side reactions leading to the undesirable decomposition of electrolytes and fading of electrode capacitance [68]. Therefore, to ensure long life span of supercapacitors, strict control of the phase purity of carbon materials are highly recommended [93].
- (5). Low-cost and green preparation process. In order to promote the development of commercial supercapacitors, the cost-effective preparation process of electrode materials is desired, which necessarily requires a wide variety of raw materials with low price from factories. In addition, the manufacturing equipments and the preparation process should be easy to be industrialized with minimum capital investment. The use of highly toxic, flammable and explosive reactants should be avoided throughout the material preparation process, and the proper post-treatment of waste materials after product preparation is also needed to achieve green recycling.

In summary, the general rule in selecting carbon-based supercapacitor electrode materials is to find a novel carbon production technology that is ideally cost effective, industrially scalable and economically attractive using renewable and abundant resources, whilst achieving energy storage performances comparable or even superior to carbon materials fabricated with existing technologies. The following sections will give a critical review of the history and present status of CO₂ conversion into various advance carbon materials.

3. Recent progresses in carbon materials prepared from carbon dioxide

Carbon dioxide is essentially an inert species with low chemical activity due to its extremely high entropy of -394 kJ mol^{-1} , and the C=O bond in CO₂ is stable with a bonding energy of 750 kJ mol^{-1} . As a result, it is not easy to break this robust chemical bond and directly convert CO₂ into carbon products without appealing to strong reductants such as Mg or alkaline metals of Li, Na. Indeed, current technologies concerning the utilization of CO₂ into carbon materials are all based on this general thread, which can be categorized into four major protocols: direct metallothermic combustion, high temperature reduction, carbonate-assisted conversion and controllable self-sustaining synthesis.

3.1. Direct metallothermic combustion with CO₂

Metallothermic reduction is a method of using metal (or its alloy) as a reducing agent to reduce a metal-based compound at

high temperature to obtain pure metal [94], which has been widely adopted in industrial metallurgical processes as well as in fabrication of novel energy-related materials including macroporous Si [95], porous carbon/metal composites [96] and hollow Ge microspheres [97]. In particular, magnesiothermic reactions are well known for their capability in dissociating robust chemical bonds, such as the Si–O bond in SiO₂ to form porous silicon nanoparticles [98] and the C–O bond to purify carbon-based materials [99]. The reaction between Mg and CO₂ proceeds according to the formula:



which has a highly spontaneous tendency and releases huge amount of heat to propel the reaction until completion. Due to this unique feature, magnesiothermic reaction has been envisaged by researchers in 1980s to supply power for combustion engines using the atmospheric CO₂ on Mars and Venus [100]. Besides, as one of the most widely distributed elements in nature (the eighth richest element in earth's crust), Mg can be facily prepared in industries with low cost and large quantities. For these reasons, the early attempts to fabricate carbon materials from CO₂ started with metallic Mg.

In 2011, Chakrabarti et al. [56] pioneered the exploration of CO₂-converted graphitic carbon materials. They ignited 3 g of Mg ribbon inside a bowl filled with dry ice, and after the combustion of Mg in CO₂ the black carbon were collected and transferred into diluted hydrogen chloride to remove the impurities. The carbon products present typical hollow nanocubic morphology with average size of 400 nm and shell thickness of 10 nm (Fig. 2a). Importantly, the Raman spectrum consists of a prominent G band at 1570 cm^{-1} and a splitting G' band at 2645 cm^{-1} (Fig. 2b), signifying that the products obtained by this method possess a high graphitized structure. The magnesiothermic process is cost-effective and can be potentially used to produce carbon materials in large quantities without the involvement of toxic chemicals, thus offering further incentives for fabrication of carbon materials with different structures and morphologies from CO₂ precursor. It should be noted that the morphological results in this work still show clearly the presence of MgO impurities deeply embedded in the carbon matrix, which are difficult to be removed completely due to the impossible wettability by hydrogen chloride during post treatment.

Following this work, Cuning et al. [101] also produced graphene nanocages via high temperature combustion of Mg in CO₂ atmosphere. The graphene samples present hollow rectangular-shaped agglomerates of nanocages with lateral size of $\sim 100 \text{ nm}$ and noticeably thick edges due to the folding of graphene sheets during combustion synthesis. These structural characteristics are unique when compared with reduced graphene oxide (RGO) samples, which usually exhibit crumpled individual sheets of microns in size [102]. One major problem for these graphene nanocages is the limited surface area of $235.5 \text{ m}^2 \text{ g}^{-1}$ due to the severe stacking of the graphene sheets into bulk graphite. The elemental analysis of the graphene sample shows 86.3 at% C and 7.0 at% O. The C/O atomic ratio of ~ 21 is considerably higher than the majority of RGO samples (~ 20 at% O) [102], which suggests the high reaction temperature enabled by the fierce combustion between Mg and CO₂ is kinetically favored to further reduce surface-bound oxygen. However, the major problem for this work is the 6.3 at% Mg (in the form of MgO) in the carbon samples, quantitatively describing that the product still contains relatively high amount of Mg-related impurities. Therefore, a modified strategy is expected to further enhance the surface area and control the elemental composition and microstructure of CO₂-converted carbon materials. Pumera et al. [103] explored the mild ignition of Li metal in solid CO₂ (dry ice) to fabricate few-layered graphene materials with high

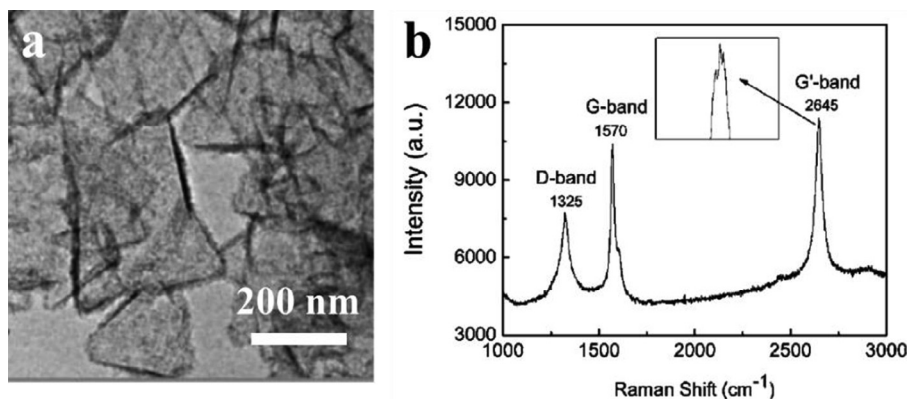


Fig. 2. (a) TEM morphology and (b) Raman spectrum of carbon products from the combustion of Mg in dry ice [56].

purity. This protocol can bypass the problem of residual metallic impurities, but the C/O ratio of only 3.53 in the products signifies a large amount of oxygen-containing groups are present on the basal plane of graphene, which is caused by the relatively low reaction temperature between Li and CO₂.

The electrochemical properties of carbon materials depend not only on the porosity but also to a large extent on the surface engineering built into their structures. It has been widely recognized that carbon materials doped with various heteroatoms (boron [104], nitrogen [105], phosphor [106], sulfur [107], etc.) exhibit unique physical and chemical properties in aqueous or organic electrolytes when the graphitic carbon atoms are properly substituted or covalently bonded by foreign atoms. For example, the charge distribution and spin density of carbon atoms can be tailored by their neighboring alien atoms, which act as numerous 'active areas' on carbon surface to improve the energy storage capability [108–110]. For this reason, the introduction of heteroatoms into carbon nanoframework during the combustion process of CO₂ conversion is worthy of study. The challenge is how to

achieve doping in this violent metallothermic combustion reaction and simultaneously avoid the collapse of carbon morphology and porosity. Zhang et al. [111] designed a burn-quench method to achieve the large-scale production of mesoporous and N-doped graphene nanosheets with controlled architecture and extensively explored their supercapacitive performances (Fig. 3a). Typically, Mg ribbon was ignited in CO₂ and then followed by in situ quenching in NH₄HCO₃ aqueous solution, which could produce approximately 1 g graphene for 25 g Mg after dissolving the remaining MgO in diluted acid. The scrolled sheet-like structure of graphene nanosheets are mostly composed of graphitic carbon. The dimensions of nanographene range from 10 nm to dozens of microns and the height is 0.8–1.2 nm, not only providing good mechanical properties but also avoiding graphene aggregation (1–5 layers). The graphene samples show an elemental composition of 92.8 at% C, 1.5 at% Mg, 4.3 at% O, and 1.4 at% N, exhibiting a low oxygen content and reasonable nitrogen doping. Nitrogen has a similar size as carbon atom and is a good electron-donor, which can enhance the reaction activity and electrical conductivity of elec-

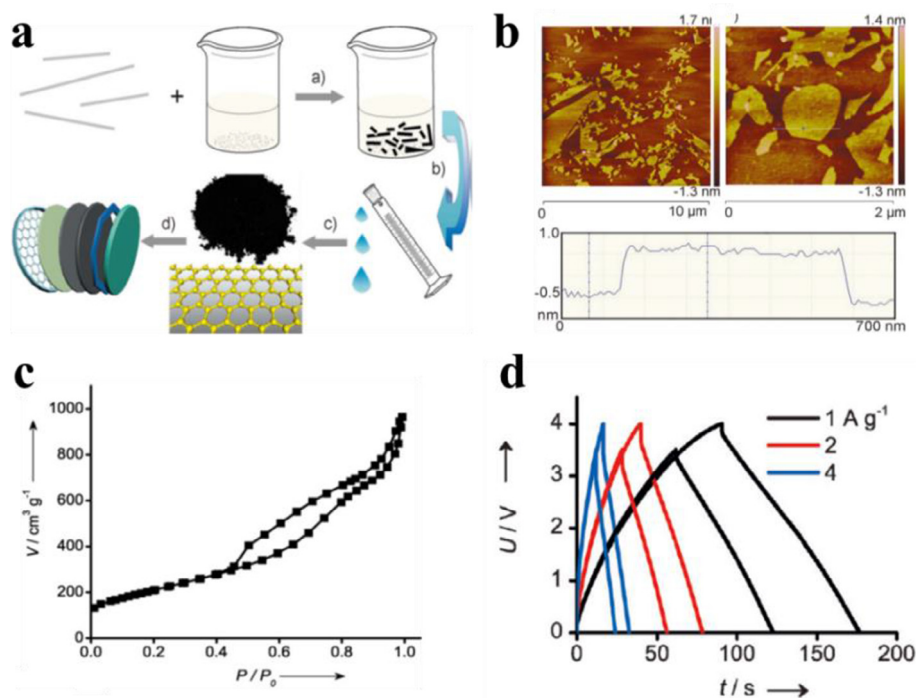


Fig. 3. (a) Schematic illustration of burn-quench method for graphene preparation and the assembly of supercapacitor cells; (b) atomic force microscopy image of the nanographene sheets on a mica substrate indicating the dimension and height; (c) N₂ adsorption–desorption isotherm of nanographene; (d) galvanostatic charge/discharge curves of symmetrical graphene-based supercapacitors under different current densities [111].

trodes through electron conjugation with carbon framework [112–114]. Encouragingly, the amount of Mg-related impurities in the carbon samples is relatively low, probably caused by some Mg or MgO particles adsorbed onto the surface or into the pores of the nanostructure. The specific surface area of graphene is substantially enhanced to $756 \text{ m}^2 \text{ g}^{-1}$ with a high pore volume of $1.5 \text{ cm}^3 \text{ g}^{-1}$ (Fig. 3c). The pore size distribution lies predominantly within 2–10 nm, which promises an unobstructed ion transportation performance. Besides, the conductivity of graphene electrode film is 150 S m^{-1} and a low inner resistance of approximately 9Ω , also ensuring a good electron transfer capability. Using ionic liquid electrolyte, the capacitance of graphene electrode reaches 95.2 F g^{-1} within a wide potential window of 4 V (Fig. 3d). It is important that 61% of the capacitance can be maintained when the scanning rate is increased 200 mV s^{-1} , which guarantees a maximum energy density and power density of 51.5 Wh kg^{-1} and 20 kW kg^{-1} . Besides, the capacitance retention is 91% after 1200 cycles at a discharge rate of 2 A g^{-1} . The lithium-ion storage capacity of graphene electrode is also evaluated. A reversible specific capacity of 666 mAh g^{-1} at a discharge current density of 0.2 A g^{-1} can be obtained. This burn-quench method is believed to contribute to the high-throughput and low-cost production of graphene materials for electrochemical energy storage applications.

The major bottleneck for the power density of commercial supercapacitors is the low conductivity of AC electrodes. Consequently, how to modify electrode materials with low cost for the improvement of their charge transfer is a research hotspot. Qin et al. [115] obtained few-layer graphene by burning Mg and Ca in CO_2 atmosphere, and used them as conductive additives for supercapacitors to enhance the rate behavior and power density of activated carbon electrode. The morphologies of the as-prepared graphene sample are superimposed cubes with sizes typically in the range of 50–200 nm as well as scrolled and entangled graphene nanolayers with fewer than five monolayers of graphene. The capacitance of graphene-modified electrodes reaches 220 F g^{-1} at 0.1 A g^{-1} in aqueous electrolyte, which still preserves 186 F g^{-1} at the current density of 2 A g^{-1} . These results are much higher than AC-based electrodes incorporated with carbon blacks or graphite powders. This work proves that graphene materials converted from CO_2 can act as highly efficient conducting agents in carbon electrodes to improve the rate and power performances.

Although direct metallothermic combustion protocol is able to convert CO_2 into carbon materials and some research progresses have been achieved in this field, the method still has several drawbacks: (1) The direct combustion reaction is violently exothermic and is usually rapid, which renders the accurate control of reaction process and specific morphology of products a tricky trouble. (2) The trace amount of MgO wrapped in the prepared carbon materials are difficult to remove by acid treatment. This leaves a threat to the full use of the electrochemical performance of carbon-based electrodes because the inert impurities contribute no capacitance but occupy 'dead mass' in the electrodes [116]. (3) The specific surface area of these carbon materials is usually low compared with commercial ACs or few-layer graphene, thus causing a limited space for efficient charge accumulation and energy storage. (4) The reducing agents may partially participate in the combustion reaction due to the fierce heat released from the system, also resulting in a low CO_2 conversion rate. It is still necessary to improve the technology to realize the controllable preparation of high-purity carbon materials converted from CO_2 .

3.2. High-temperature reduction in CO_2 flow

High-temperature reduction has been developed as a more mature preparation method in the past few years to controllably reduce CO_2 gas into carbon materials with specific morphology

and pore structure. The core idea of this protocol is the reaction between strong reductants and CO_2 in a tube furnace at high temperature. The reaction kinetics can be facilely changed by adjusting the reaction temperature, gas flow speed and reaction time to achieve a controllable conversion of CO_2 . Zhang et al. [117] proposed a high-temperature magnesiothermic reduction for the first time to synthesize nanocarbons with controlled shape using the reaction of Mg powder with CO_2 gas in a furnace (Fig. 4a). The melting point and boiling point of Mg is 648 and 1090 °C, respectively; therefore, by simply regulating the furnace temperature, novel carbon nanostructures can be obtained based on different interfacial phase reaction mechanisms. At a temperature of 600 °C, the solid/gas interface between Mg and CO_2 is beneficial for the absorption and rearrangement of carbon atoms on the top surface of MgO to form graphene layer for the minimization of free energy. The MgO template also regulates the porosity evolution to produce mesoporous graphene (MPG) (Fig. 4b, c). At an elevated temperature of 800 °C, the CO_2 decomposition is driven by the capillary surface tension of Mg liquid phase to form carbon tubular nanostructures (CTN) (Fig. 4d and e). When the temperature is further increased to 1000 °C, the cubic lattice of MgO particle during reaction serves as a self-generated template to shape the encapsulated growth into hollow carbon nanoboxes (HCB) (Fig. 4f and g). The electrochemical performances of these carbon materials are essentially morphology-dependent. In organic electrolytes, the capacitance of MPG, CTN and HCB at 0.2 A g^{-1} is 150, 87 and 75 F g^{-1} , respectively. In particular, a high capacitance of 110 F g^{-1} for MPG can be achieved even at a high current density of 10 A g^{-1} , and after 5000 cycles the capacitance retention is still as high as 92%. When ionic liquid is adopted as electrolyte, the maximum energy density of MPG is 80 Wh kg^{-1} within a wide operating voltage window of 4 V (Fig. 4h–j). Moreover, the nanocarbon electrodes also present a high lithium storage capacity of $\sim 1100 \text{ mAh g}^{-1}$ because the nanostructure with high surface can adsorb enough solvated lithium ions to the surface and edge to enhance capacity at high potential [118]. This work provides a novel approach for efficient process for CO_2 sequestration and synthesis of carbon materials with controlled morphology for energy storage.

Shortly after this work, a modified high-temperature magnesiothermic reduction has been developed by Ji et al. [119] to prepare porous graphene materials with high specific surface area, which involves the controlled reaction between the mixture of Mg/Zn powder and CO_2 at 600 °C (Fig. 5a). They investigated the reaction temperature, the flow rate of CO_2 gas and the Mg/Zn mass ratio on the degree of graphitization and specific surface area of the product, which reflect the dual-role of Zn in carbon formation and activation (Fig. 5b and c). The as-prepared porous grapheme shows a high specific surface area of $1900 \text{ m}^2 \text{ g}^{-1}$ and a good electrical conductivity of 1050 S cm^{-1} , which can offer sufficient accessible area for electrolyte ions and electron transportation capability. As expected, quasi-rectangular CV curve of graphene-based electrode demonstrates a quick response in capacitive energy storage (Fig. 5d). A high specific capacitance of 190 F g^{-1} at 10 A g^{-1} and quick rate capability in aqueous KOH electrolyte can be reached (Fig. 5e) together with a good capacitance retention of 98% after 10,000 cycles. The importance of this new strategy lies in the controlled conversion of CO_2 into porous carbon materials with both high specific surface area and high electrical conductivity as superior electrodes, rendering them great affordability and scalability in high-performance supercapacitors.

It has long been recognized that Ni can serve as efficient catalyst adjust the growth of carbon nanotubes and graphene [120,121], which promotes the investigation of its role in the magnesiothermic reactions of CO_2 . Wang et al. [122] reported the direct synthesis of 3D carbon nanotube foam (CNTF) macrostructure with the

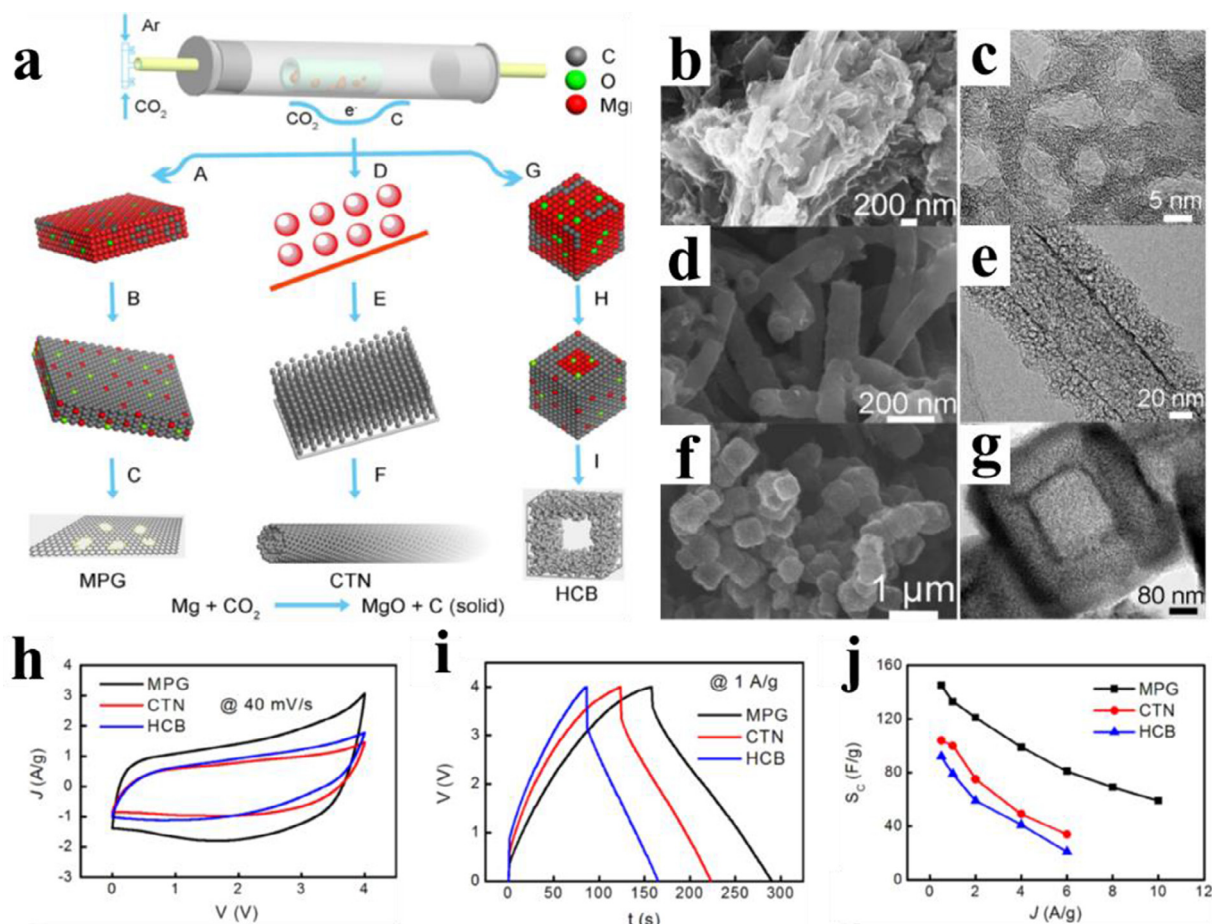
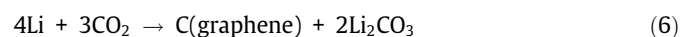


Fig. 4. (a) Formation mechanism of nanocarbons; (b, c) TEM and SEM images showing the sheet-like and scrolled morphology of MPG; (d, e) tubular microstructure of CTN; (f, g) cubic morphology of HCB; (h) CV curves of nanocarbons at 40 mV s⁻¹ between 0–4 V; (i) charge/discharge curves of nanocarbons at a current density of 1 A g⁻¹; (j) rate capability of nanocarbons various current densities [117].

catalysis of nickel foam through a template-directed high-temperature reduction of CO₂, which has advantages of light mass, good electrical conductivity and high surface area. The CNTF is further used as scaffold to deposit electrochemically active Ni(OH)₂ to fabricate composite electrode with a specific capacitance of 259 and 131 F g⁻¹ at a current densities of 0.5 and 10 A g⁻¹, respectively. Meanwhile, the electrode also exhibits excellent long-term stability with a 94% capacitance retention after 2000 cycles because the robust CNTF scaffold accommodates the volume change of Ni(OH)₂ during cycling tests. This facile and cost-effective synthetic method can also be extended to fabrication of other electroactive materials supported by carbon scaffold and promote their application in advanced energy storage. Recently, Lee et al. [61] introduced a one-pot synthesis of graphene materials grafted by carbon nanofibers using Ni powder as catalysts to regulate the morphology of carbon products during CO₂ conversion. They found that Ni exerted a crucial role in regulating the microstructure of products because it can offer new nucleation sites for nanofiber growth. The carbon products achieve a high capacity of 820 mAh g⁻¹ after 100 cycles at 0.5C when used as cathodes in Li-S batteries.

Except Mg as successful reductant, researchers found that some materials with strong reducing effect could also react with CO₂ under elevated temperature. Lou et al. [123] first synthesized carbon nanotubes (55 nm × 1.5 μm) by the reduction of supercritical state CO₂ with metallic lithium at 550 °C, 700 atm for 10 h. However, the high pressure in the reaction system prohibits the possibility for mass production and easy affordability of carbon

materials. To achieve mild reaction conditions, Hu et al. [124,125] obtained cauliflower-fungus-like graphene (CFG) from a one-step reaction between Li liquid and CO₂ gas in a furnace at 550 °C and atmospheric pressure according to the equation (6):



which is thermodynamically favorable for graphene formation because of the negative Gibbs free energy change (−1081 kJ mol⁻¹) and enthalpy change (−1260 kJ mol⁻¹). The Li₂CO₃ in the system can control the growth of graphene and separate graphene sheets, ensuring a high specific surface area of 462 m² g⁻¹ and a hierarchical mesoporous and microporous distribution within the range of 2–70 nm. This microstructure can allow electrolyte molecules to easily shuttle into the CFG electrode bulk and thus contact the internal surface for the improvement of electron/ion transportation capability. Even with a high mass loading of ~11 mg cm⁻², the CFG electrode still provides a large capacitance of 103 F g⁻¹ and an ultrahigh areal capacitance of 1.16 F cm⁻² at a current density of 1 A g⁻¹. However, a major challenge for Li as reducing agent is its high reactivity in moisture atmosphere. The oxygen and H₂O level in equipment must be kept very low to prevent the undesired oxidation of Li, which make it rather hard to accurately control the repeatability of each preparation batch. Several other chemically stable reductants are also tried. Chu et al. [126] developed a chemical vapor deposition method using Fe, Ni-based composites to assist the catalytic conversion of CO₂ into solid-form carbon materials. He et al. [58] prepared graphitic carbon nanosheets (GCNSs)

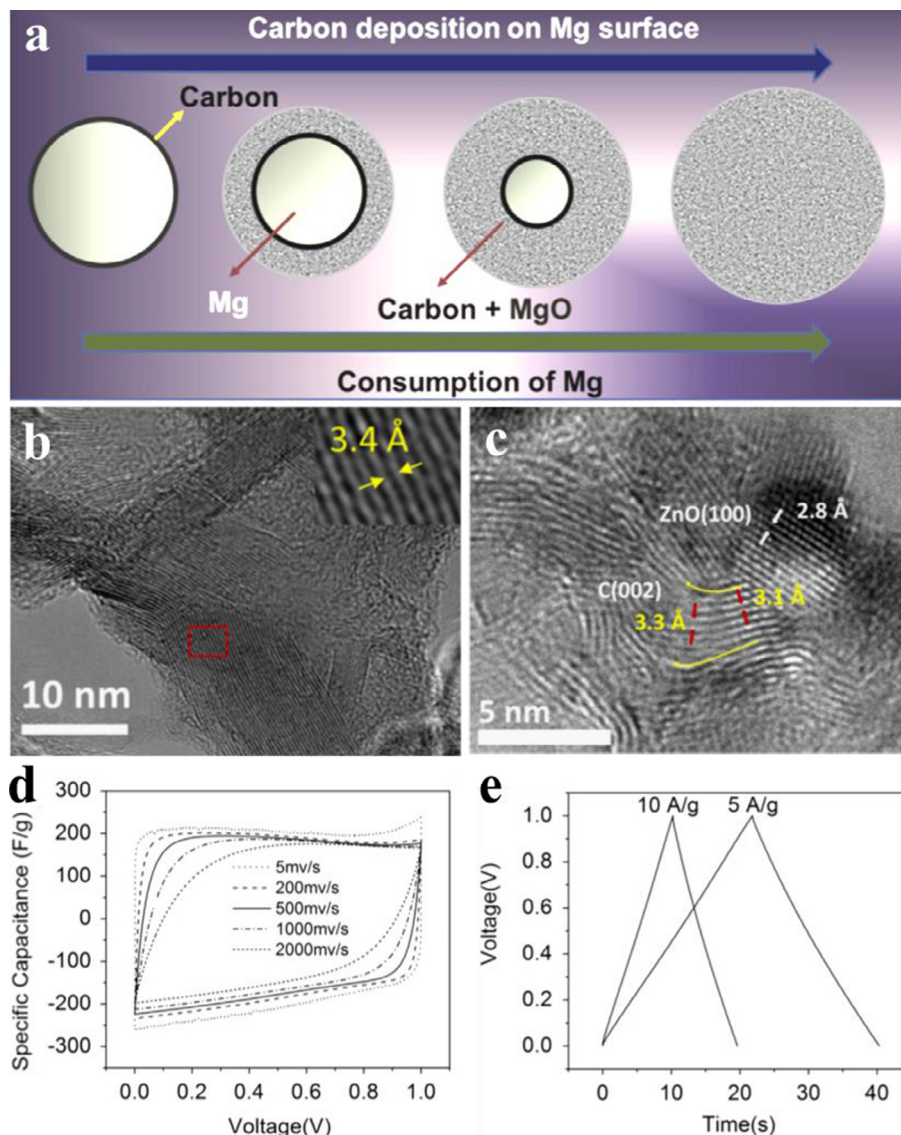


Fig. 5. (a) Scheme of carbon deposition at the surface of molten Mg droplet during reaction; (b) magnified TEM images of porous graphene; (c) epitaxial growth of graphene on the surface of ZnO; (d) CV curves of graphene electrode at different sweeping rates in aqueous electrolyte; (e) galvanostatic charge/discharge curves recorded at current densities of 5 A g^{-1} and 10 A g^{-1} [119].

through a thermal reaction between CO_2 and calcium carbide (CaC_2). The GCNSs exhibit cambered and crumpled structures with a thickness of 10–50 nm and lateral size of several microns, which could deliver an initial reversible lithium-ion storage capacity of 513 mAh g^{-1} at 100 mAh g^{-1} and a good rate performance with a reversible capacity of 293 mAh g^{-1} at 1 A g^{-1} .

Doping of carbon materials by high-temperature reduction technology has been explored by Zhang et al. [57] to realize a higher electrochemical reactivity. They investigated the reaction of CO_2 with ammonia borane (NH_3BH_3), which includes CO_2 fixation at moderate temperature and subsequent graphitization in the temperature range of 600–750 °C. The final product is boron-doped graphene oxide flakes with thickness of less than 6 nm (Fig. 6a). Several porous boron-doped carbon nanostructures (Fig. 6b) were also constructed using the reaction between sodium borohydride (NaBH_4) and CO_2 at 500 °C and atmospheric pressure [127–129]. The carbon products were then subjected to chemical activation by KOH to increase the specific surface area from ~ 360 to $1800 \text{ m}^2 \text{ g}^{-1}$ with a total pore volume of $1.2 \text{ cm}^3 \text{ g}^{-1}$. These boron heteroatoms in the carbon enhance the electrochemical performance by generating pseudocapacitance and modifying the

electronic structure, which can be revealed from the nearly unchanged specific capacitance of $130\text{--}140 \text{ F g}^{-1}$ as the discharge current density increases from 1.35 to 6.76 A g^{-1} in $1 \text{ M Na}_2\text{SO}_4$ electrolyte (Fig. 6c and d). In addition, a good capacitance retention of 93% can be achieved after 3510 cycles at 3.3 A g^{-1} .

It should be noted that the high-temperature reduction technology still faces several bottlenecks for carbon material fabrication. Indeed, this technique can controllably convert CO_2 gas into carbon materials with specific morphology and pore structure; however, it requires a huge amount of energy input during the reaction process and a lengthy reaction time, making it difficult for industrial-scale applications. In addition, since the reaction temperature in the furnace is usually set around 600–1000 °C, the crystallinity and electrical conductivity of carbon products still need further improvement to enhance the energy and power density.

3.3. Carbonate-assisted conversion of CO_2

Another method for preparing carbon materials is to utilize different carbonates as the CO_2 source and the gas released by the decomposition of carbonates at high temperature react with Mg to

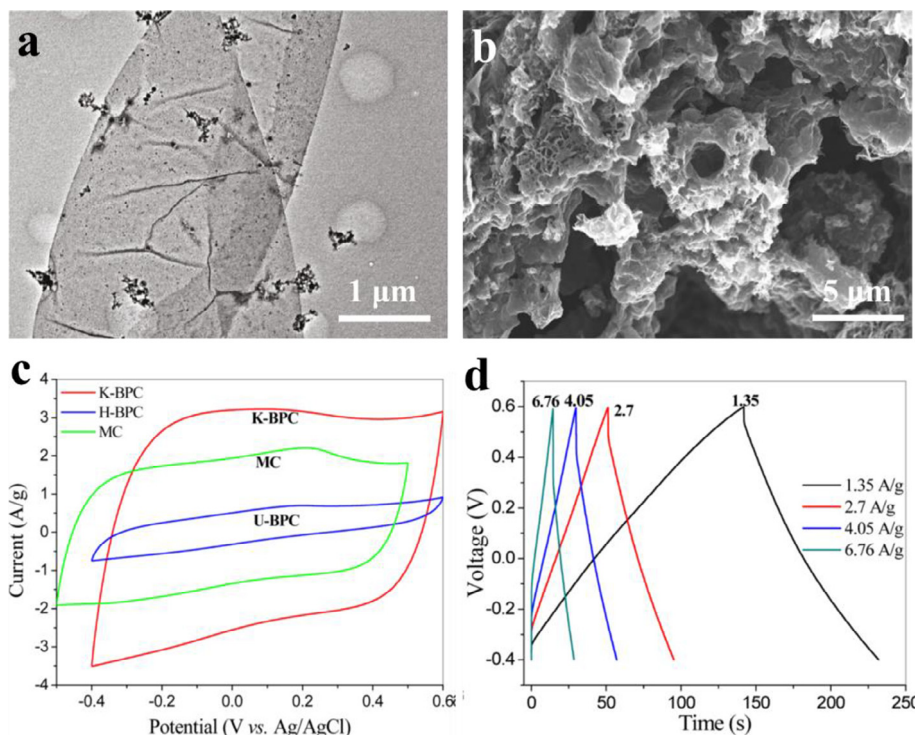
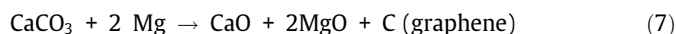


Fig. 6. (a) TEM images of boron-doped graphene flakes using NH_3BH_3 as reducing agent [57]; (b) representative SEM image of boron-doped porous carbon by the reaction of carbon dioxide with sodium borohydride [127]; (c) CV curves and (d) charge/discharge profiles of boron-doped porous carbons in 1 M Na_2SO_4 electrolyte [128].

form carbon-based materials, which can be treated as a variant of high-temperature reduction technology. Tang et al. [130] showed that graphene nanosheets could be synthesized from eggshell by a high-temperature magnesiothermic reduction reaction at 700 °C:



They found that the key factor influencing carbon formation is the higher equilibrium pressure of CO_2 released from the decomposition of CaCO_3 than the equilibrium vapor pressure of magnesium at a specific temperature range. The graphene nanosheets presents a typical porous microstructure with a thickness of less than 10 nm, a specific surface area of $551 \text{ m}^2 \text{ g}^{-1}$ and a C/O atomic

ratio of 17, larger than most chemically reduced graphene materials. The lithium-storage properties of the obtained graphene products show a reversible capacity of 678 mAh g^{-1} at a specific current of 100 mA g^{-1} . More importantly, after 1000 charge/discharge cycles, the reversible capacity still retains 150 mAh g^{-1} at a high current density of 20 A g^{-1} . Similarly, Liang et al. [131,132] fabricated toast-like porous carbons (TPC) via a one-step solid reaction between LiH and CaCO_3 at 600 °C (Fig. 7):

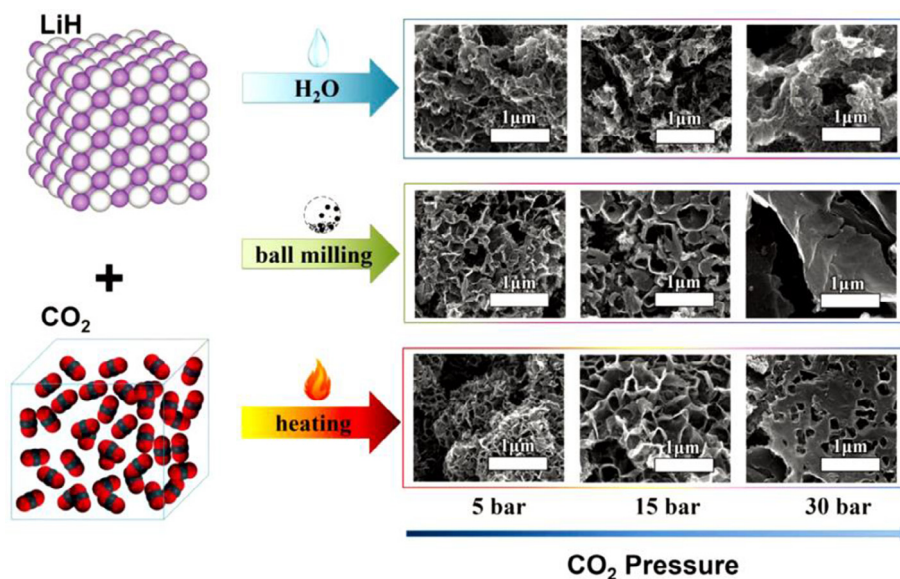
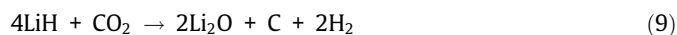


Fig. 7. Schematic illustration of LiH-assisted CO_2 conversion into nanocarbons via various techniques, including water introducing, heating, and ball milling [132].

The release rate of CO_2 gas from the temperature-induced decomposition of CaCO_3 plays a key role in the guided formation of carbon products. The specific surface area of $601.4 \text{ m}^2 \text{ g}^{-1}$ and micro/mesoporous structure of TPC gives rise to enough electrode/electrolyte interfaces for charge storage, displaying an ultra-high specific capacity of 1016 mAh g^{-1} at 0.2 A g^{-1} , a superior rate capability of 730 mAh g^{-1} at 1 A g^{-1} and an excellent cycling stability up to 1400 cycles at 4 A g^{-1} . Such a good electrochemical behavior makes TPC a promising candidate as high-power electrode materials especially in lithium-ion hybrid supercapacitors.

Heteroatom-doped carbon materials can also be designed by carbonate-assisted conversion. Wang et al. [133] prepared sulfur-doped graphene (SG) by a magnesiothermic reduction in the temperature of $700\text{--}900 \text{ }^\circ\text{C}$ using low-cost Na_2CO_3 and Na_2SO_4 as carbon and sulfur sources, respectively (Fig. 8a). The reaction mechanism at high temperature involves the reduction of CO_3^{2-} in Na_2CO_3 by Mg and the in-situ reactive hybridization of sulfur in SO_4^{2-} into the sp^2 carbon framework, which can provide a S doping of 1.8 at%–2.6 at% depending on the amount of Na_2SO_4 in the system and temperature. The resulting SG demonstrates a typical crumpled and porous structure with sp^2 -hybridized layer number of less than 10 layers (Fig. 8b–d). This morphology is very different

from the graphene prepared using CaCO_3 as the carbon source, suggesting the introduction of sulfate salt in the reaction system significantly changes the microstructure of graphene. SG shows a specific surface area of $\sim 190 \text{ m}^2 \text{ g}^{-1}$, a pore volume of $1.4\text{--}1.6 \text{ cm}^3 \text{ g}^{-1}$ and an unimodal mesopore distribution at 3.8 nm , which are comparable to N-doped thermally reduced GO [134]. The present magnesiothermic reduction procedure is also promising to prepare other heteroatom-doped (P, N and B) graphene materials for batteries or supercapacitors.

Kim et al. [62] proposed a nano-templated CO_2 conversion for boron-doped porous carbon with good capacitive behaviors. The mixture of NaBH_4 mechanically mixed with CaCO_3 was heated to $500 \text{ }^\circ\text{C}$ under CO_2 flow for 2 h, and the products were hierarchical porous carbon nanosheets with high specific surface area of $1262 \text{ m}^2 \text{ g}^{-1}$ and adjustable boron doping level of 0.5 at%–2.2 at%. An excellent capacitance of 270 F g^{-1} at 1 A g^{-1} can be obtained in aqueous electrolyte, which still retains up to 170 F g^{-1} when the current density is increased to 20 A g^{-1} .

A special shock wave method was proposed by Yin et al. [135] to transform carbonate into multilayer N-doped graphene (NG) using ammonium nitrate (NH_4NO_3) as nitrogen source, which is conducted by giving the mixture of CaCO_3 and Mg an instanta-

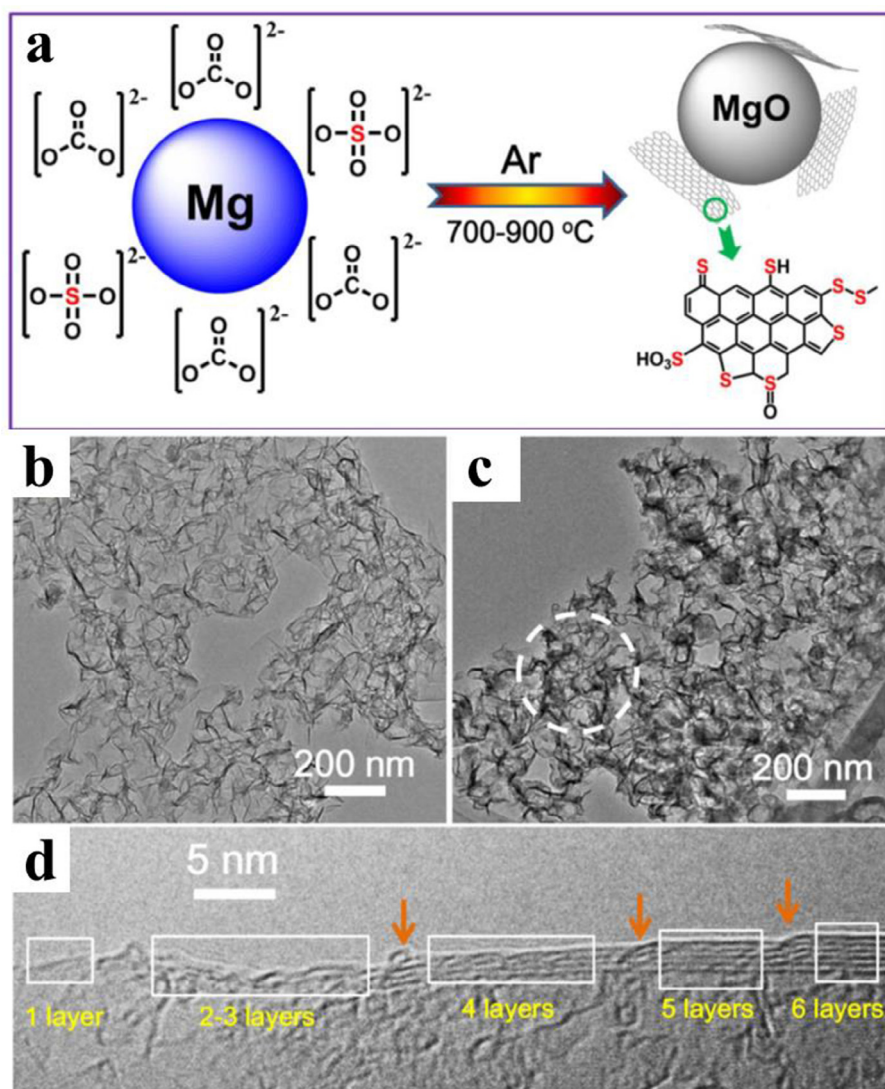


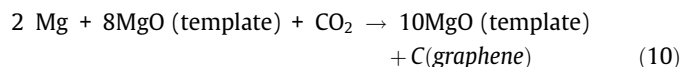
Fig. 8. (a) The schematic illustration implying the production of S-doped graphene by magnesiothermic reduction of Na_2CO_3 and Na_2SO_4 ; (b–d) TEM images of S-doped graphene showing the few-layer feature [133].

neous shock wave by a detonation-driven flyer. This shock-wave action generates a rapid and non-equilibrium process inducing high temperature, high pressure and high strain rate in the system. Under these extreme conditions, CaCO_3 disintegrates into CO_2 and CaO to promote the simultaneous reaction between CO_2 and Mg , and the nitrogen atoms released from the decomposition of NH_4NO_3 form a robust chemical bond with the carbon atoms. The NG products show very thin curved and loose film-like morphology with well-defined graphitic edges and interlayer distance of 0.3–0.4 nm. The N/C atomic ratio in the NG sample is calculated to be 3.84%. This protocol can achieve quick preparation of graphene materials, but the explosive ammonium nitrate used in the reaction process might induce danger during the operation, which seems difficult to be applied for large-scale industrialization.

3.4. Controllable self-sustaining reaction with CO_2

Although the above CO_2 reduction protocols have made great progresses in preparing numerous carbon materials, important problems still exist in the convenience of reaction process, energy cost and product quality control, which limit them mainly in laboratory for experimental and characterization applications. It is still urgently desired to develop a straightforward and environment-friendly technique for industrial manufacturing of high-quality carbon materials directly from CO_2 . Since the pioneering work of Merzhanov et al. [136] in 1960s, a self-sustaining reaction called self-propagating high-temperature synthesis (SHS) has received much attention from both academia and industry as a novel protocol to manufacture useful ceramics [137,138], intermetallics [139], refractory materials [138], and thermoelectric materials [140,141]. The foremost feature of SHS technique is an essentially exothermic reaction ignited by a small amount of energy input to one part of the system, then the released heat is sufficient to generate a combustion wave that spontaneously propagates in a self-sustaining manner throughout the remaining parts of the reaction system. Due to the fierce heat release from the reaction between Mg and CO_2 , it is possible to realize the conversion of CO_2 into carbon materials by SHS technique; the point is how to proceed the reaction controllably under extreme high temperature to prepare carbon materials with designed microstructure and high purity.

A controllable and scalable SHS strategy is proposed by our group to convert CO_2 into high-quality SHS-prepared graphene (SHSG) with low cost and environmental friendliness (Fig. 9a) [142]. Briefly, in a reaction chamber filled with CO_2 , a mixture of Mg and MgO powders with a prefixed mass ratio is given an electricity-induced heat input, which is ignited and proceeds in a self-propagating manner till completion according to the following formula:



The whole reaction takes only a few seconds. The simple post-treatment involved the removal of MgO template by hydrochloric acid and freeze-drying of grapheme products. The MgO in the initial system exerts a crucial effect on the microstructure of carbon products (Fig. 9b). A higher MgO/Mg mass ratio results in loosely stacked graphene nanosheets (<5 layers) due to the sufficient growth space provided by MgO templates, while a low ratio causes hollow graphene cages with thicker layers because of the rapid growth rate of graphene on cubic MgO crystal surface. Li et al. [143] also adopted SHS technique to manufacture graphene materials and validated that the content of the MgO diluent has an important influence on the morphology, crystallinity and surface properties. The typical microstructure of SHSG is composed of

interconnected few-layer graphene (Fig. 9c and d), which is integrated into intertwined scaffolds to provide porous space between adjacent layers. The abundant ripples and crumples of SHSG is helpful to overcome the unfavorable restacking of graphene sheets (Fig. 9e). The well-resolved in-plane carbon atoms also validate the graphitic honeycomb structure of SHSG (Fig. 9f). Theoretical calculations on the thermodynamic features of SHS system also reveal that the adiabatic temperature can be tuned from 6000 to 1800 K by changing the amount of inert MgO in the system. The SHS-prepared graphene (SHSG) nanosheets display a good electrical conductivity of $13,000 \text{ S m}^{-1}$, large specific surface area of $709 \text{ m}^2 \text{ g}^{-1}$, high C/O atomic ratio of 82 and abundant mesoporosity of $1.52 \text{ cm}^3 \text{ g}^{-1}$, which makes them ideal candidate as high-performance electrode materials for supercapacitors. Electrochemical characterization demonstrates a capacitance up to 244 F g^{-1} can be achieved by SHSG in ionic liquid electrode within a wide working voltage window of 4 V (Fig. 9g and h), which guarantees a maximum energy density of 135.6 Wh kg^{-1} at a power density of 10 kW kg^{-1} . Moreover, when the current density is increased to 500 A g^{-1} , the capacitance of SHSG can still retain 113 F g^{-1} (Fig. 9i). This outstanding rate performance also give rise to an excellent energy density of 60 Wh kg^{-1} even at an ultrahigh power density of 1000 kW kg^{-1} , which is among the best reported values in graphene-based materials (Fig. 9j). Impressively, SHSG can maintain over 90% of the initial capacitance after one million cycles at 100 A g^{-1} (Fig. 9k), indicating its high purity induces no significant side reactions during the life span of electrode. The SHS technique provides a new avenue for large-scale manufacturing of graphene materials with significantly improved overall electrochemical performances for next-generation supercapacitors.

Recently, a novel hybrid capacitor system, lithium ion capacitor (LIC), has been proposed to further boost the energy performance by employing a faradic anode and a capacitive cathode (Fig. 10a). Contrasting with conventional symmetric supercapacitors, the cathodes and anodes of LICs work within different electrochemical potential ranges [144–147]. In the charge process, Li ions intercalates into anode to decrease the potential in this battery-type electrode, while anions are transported to the surface of cathode to elevate the voltage of this capacitor-type electrode [148,149]. The opposite situation of ion movement happens in the discharge process. For SHSG, the large surface area provides high charge storage capacity while the outstanding electrical conductivity of the electrode should suppress the ohmic resistance at high current densities. These features determine SHSG can be used as high-capacity anode materials for lithium-ion capacitors [150]. The SHSG anode exhibits a typical capacitive behavior because the available surface area and mesoporosity of graphene contribute to the efficient adsorption of electrolyte ions on its surface, thus achieving a sizeable energy-storage capability at the electrolyte/electrode interface. A high specific capacity of 854 mAh g^{-1} can be obtained for SHSG anode at the charge–discharge rate of 0.4 C ($1 \text{ C} = 372 \text{ mA g}^{-1}$) with a high coulombic efficiency of >98% (Fig. 10b). The excellent electrical conductivity of SHSG is a prerequisite for fast electron transport in the graphene layers, guaranteeing a capacity of 333 mAh g^{-1} even at the high discharge rate of 10 C (Fig. 10c). Using SHSG as anode and nitrogen-doped activated carbon as cathode, the lithium-ion capacitor exhibits a maximum energy density of 146 Wh kg^{-1} and an ultra-high power density of 52 kW kg^{-1} . Moreover, an outstanding capacitance retention of 91% can be achieved after 40,000 cycles (Fig. 10d, e). This work confirms that graphene with tailored microstructure is effective to boost both the power density and cyclic life of hybrid supercapacitors.

Compared with traditional protocols for carbon material preparation, SHS boasts several special advantages: (1) One significant feature of SHS is a very short reaction time (usually in seconds)

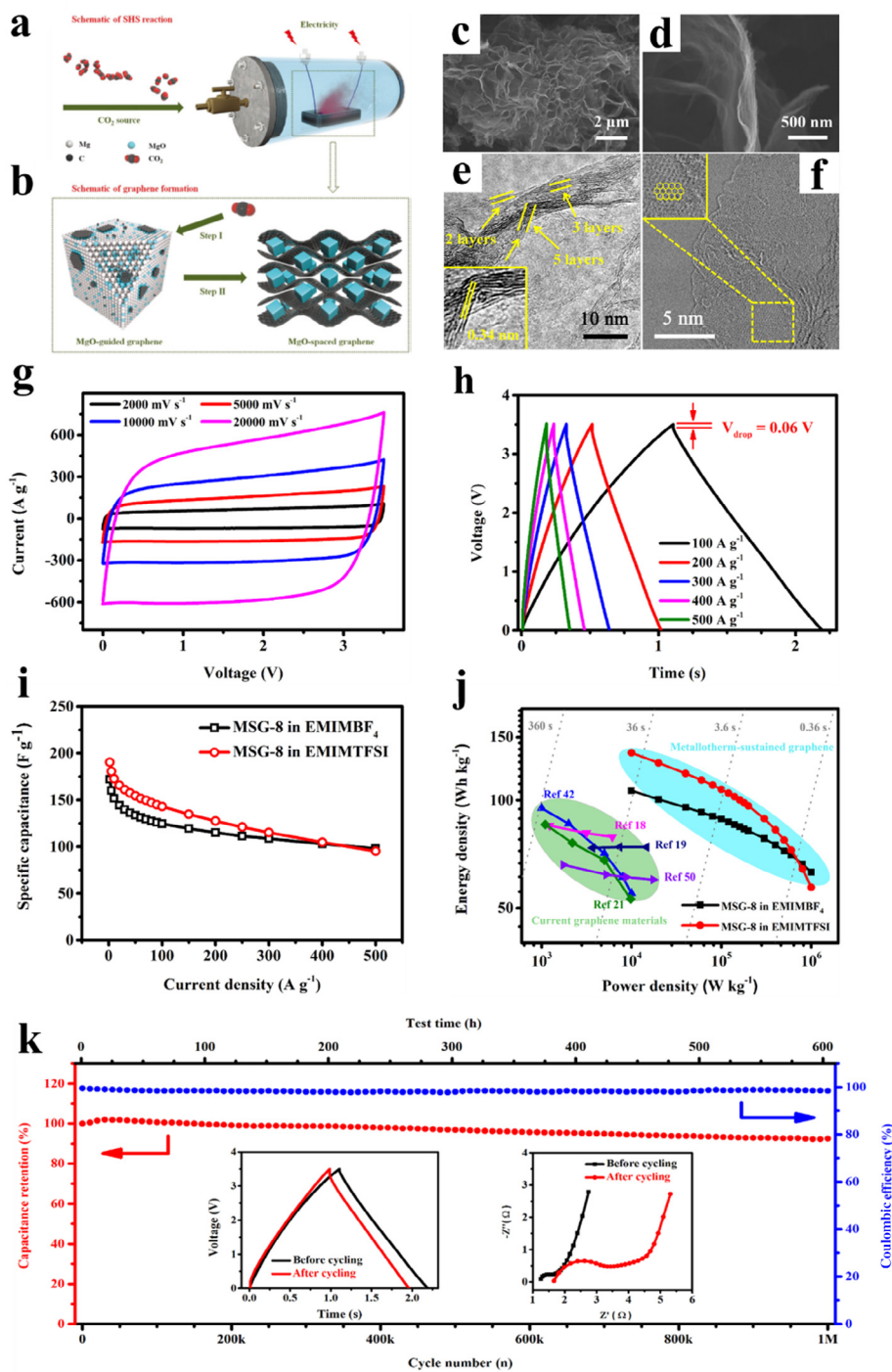


Fig. 9. (a) Schematic illustration of the SHS process; (b) the dual role of MgO in forming few-layered graphene; (c, d) SEM image, (e) TEM and (f) HR-TEM of SHSG; (g) CV curves of SHSG at scan rates from 2 to 20 V s⁻¹ in ionic liquid; (h) charge/discharge profiles of SHSG at current densities from 100 to 500 A g⁻¹; (i) Ragone plot, (j) rate performance and (k) electrochemical stability of SHSG after 1 million cycles at 100 A g⁻¹ [142].

because the heat released by the reaction is huge enough to give driving force to the combustion wave with a velocity as high as 20 cm s⁻¹. (2) SHS requires no external heating power except the minimum energy consumption in the initial ignition, which can exclude complicated energy supply equipment. (3) The heat release and transmission rate of SHS can be regulated by introducing certain inert additives in the system, making it facile to control the combustion wave velocity, temperature gradient, and material conversion rate and product structure. (4) The high adiabatic tem-

perature of SHS up to 5000 K during the reaction process is helpful to expel volatile impurities and enhance the product purity and crystallinity. (5) For large-scale production in industries, the equipment for SHS is not complicated, and the quality of the prepared carbon products is often improved with the expansion of production scale. In summary, the combination of these characteristics above determines that SHS is an efficient method for preparing high-performance carbon materials, which is expected to be widely applicable in energy storage fields in the future.

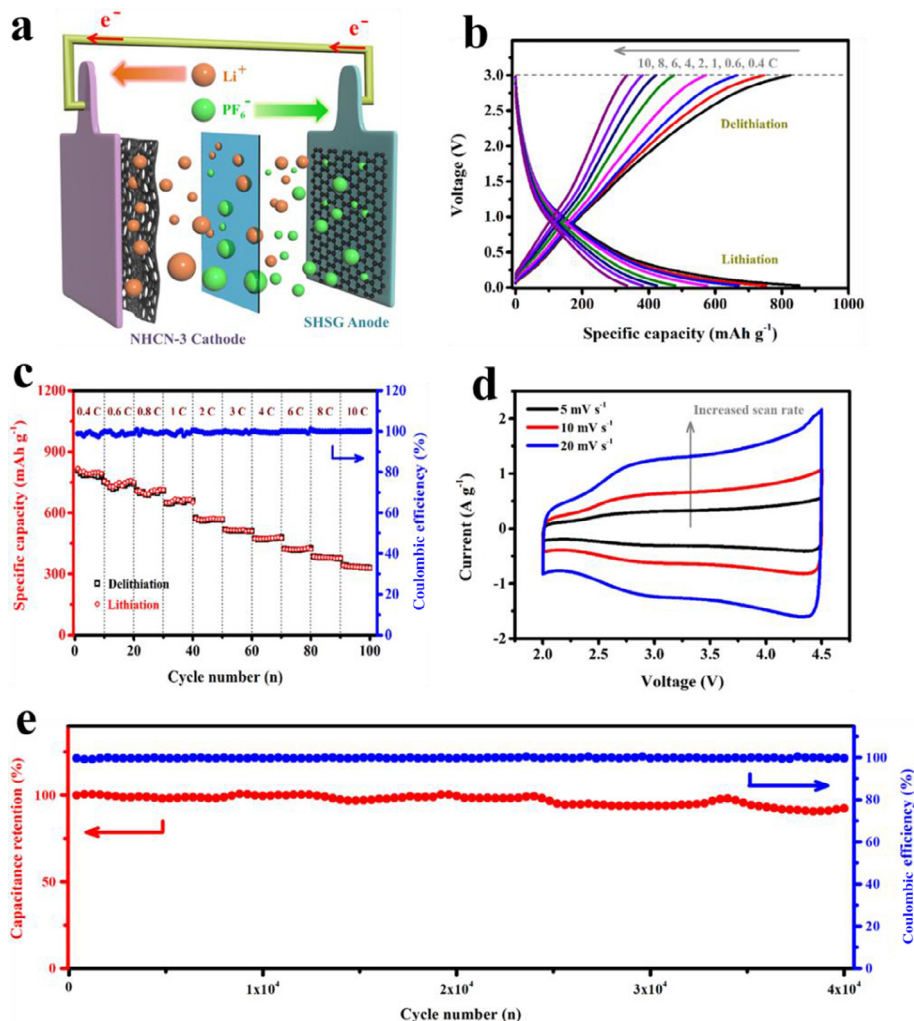


Fig. 10. (a) Schematic illustration of energy-storage mechanism of LIC based on SHSG anode; (b) charge/discharge profiles and (c) rate performance of SHSG anode from 0.4 to 10C; (d) CV profiles of LIC using SHSG anode and N-doped porous carbon cathode within the voltage range of 2–4.5 V; (e) cyclic stability of NHCN//SHSG at the current density of 4 A g^{-1} for 40,000 cycles [150].

4. Conclusions and future perspectives

The research and development of advanced carbon-based electrode materials is expected to bring important breakthrough in the next-generation high-performance supercapacitors. Indeed, the preparation of various carbon materials based on CO_2 conversion technology has been intensively studied in recent years, and has already been recognized as mature strategies for green construction of electrode materials with promising application prospects. Up till now, different methods have been proposed in this area including direct metallothermic combustion, carbonate-assisted conversion, high-temperature reduction and controllable self-sustaining reaction, which all serve to tackle the present bottleneck of low energy density for state-of-the-art supercapacitors and promote their application in the field of energy storage where repetitive fast energy storage/release is required. However, each method has its own advantages and shortcomings in terms of preparation efficiency, energy consumption, product quality, etc. Therefore, the technology details should always make corresponding improvements to target at these issues. In our opinion, the future research on CO_2 conversion into carbon materials could focus on the following aspects:

- (1). Due to the low cost of raw CO_2 , new technologies to achieve industrial-scale conversion of CO_2 into carbon are expected to significantly reduce the price of commercial electrodes, thereby bringing new opportunities for the market of carbon-based supercapacitors. One major problem is that these CO_2 conversion technologies are mostly still in the infancy of lab-scale, and large-scale manufacturing for industrial purposes is still under progress. This requires the joint effort by both academia and industry to promote the technology from lab to mature products in factories. Innovation in chemical engineering design, processing technology and manufacture equipment is essential to achieve efficient CO_2 conversion, including the precise control of thermodynamics and kinetics of reaction to obtain carbon materials with specific physiochemical properties, design of feasible industrialized machinery to reduce the preparation cost and time, and recycling of waste materials during production to meet the increasingly stringent environment regulations.
- (2). Carbon electrode materials converted from CO_2 with high capacitance, good electrical conductivity and cyclic stability are required to significantly boost the capacity and energy

density of the device. The energy storage of carbon-based supercapacitors mainly relies on the electric double layer across the electrode/electrolyte interface, which necessitates a high accessible surface area to provide sufficient locations for charge storage and generate high capacitance. On the other hand, the power capability is highly dependent on the electrical conductivity because the energy discharge rate is directly influenced by the internal resistance. However, an 'either-or' paradox exists. Materials with high specific surface area are usually accompanied with poor electrical conductivity [151]. This phenomenon is caused by the complicated pore channels in the interior of materials, which destroy the structural integrity and increase the intra-particle resistance [152]. Thus the efficiency of electron transportation across the electrode bulk is greatly inhibited. Another challenge is the proper surface engineering of carbon materials. Although various doped carbon nanostructures have been successfully fabricated from CO₂ precursor with enhanced electrical conductivity and capacitance, these heteroatoms tend to compromise the cycling performance in some scenarios due to their high reactivity with electrolytes [153]. Many efforts are expected to seek detailed kinetic and thermodynamic explanation of carbon formation chemistries and doping principles during CO₂ conversion.

- (3). The structure and configuration of carbon-based supercapacitor needs innovation to better support the practical application of novel carbon nanostructures and CO₂ conversion technology. New electrolytes with low viscosity and high conductivity should be tried in order to further improve the upper voltage limit of device, including high-voltage aqueous electrolytes, various organic solvents and conducting salts or modified aprotic ionic liquids or gel polymer electrolytes with higher ionic conductivity of ($\sim 10^{-4}$ – 10^{-1} S cm⁻¹) for flexible energy storage [147,154–155]. In this case, the proper densification of carbon materials on thick electrodes should be taken into serious consideration, which should ensure both surface utilization and pore interconnection of active materials to effectively promote the volumetric energy storage level of device [156].

In conclusion, research efforts into novel carbon nanostructures enabled by CO₂ conversion technologies will likely expand further over time because of the strong demands worldwide toward environmentally friendly and sustainable energy storage. Therefore, in spite of the present scientific and technical challenges, the CO₂-converted carbons may become promising candidates for high-capacitance, high-rate, low-cost and large-scale electrode materials in future supercapacitors. The authors believe that new upcoming experimental developments together with engineering methodologies should help overcome such obstacles in the progresses of CO₂ conversion technologies for carbon materials.

Declaration of Competing Interest

The authors declare that they have no known competing financial interests or personal relationships that could have appeared to influence the work reported in this paper.

Acknowledgments

This work was financially supported by the National Natural Science Foundation of China (No. 51907193 and No. 51677182), the Dalian National Laboratory (DNL) for Clean Energy Cooperation Fund, CAS (No. DNL201915 and No. DNL201912), the Beijing Municipal Science and Technology Commission (No.

Z181100000118006), the Key Research Program of Frontier Sciences, CAS (No. ZDBS-LY-JSC047), and the Youth Innovation Promotion Association, CAS (No. 2020000022).

References

- [1] G. Crabtree, *Nature* 526 (2015) S92.
- [2] S.L. Chou, S.X. Dou, *Adv. Mater.* 29 (2017) 1705871.
- [3] D. Larcher, J.M. Tarascon, *Nat. Chem.* 7 (2015) 19–29.
- [4] N. Armario, V. Balzani, *Energy Environ. Sci.* 4 (2011) 3193–3222.
- [5] B. Dunn, H. Kamath, J.M. Tarascon, *Science* 334 (2011) 928–935.
- [6] Y. Gogotsi, *Nature* 509 (2014) 568–570.
- [7] X.Q. Zhang, X.B. Cheng, Q. Zhang, *J. Energy Chem.* 25 (2016) 967–984.
- [8] J.B. Goodenough, K.S. Park, *J. Am. Chem. Soc.* 135 (2013) 1167–1176.
- [9] N. Nitta, F.X. Wu, J.T. Lee, G. Yushin, *Mater. Today* 18 (2015) 252–264.
- [10] F. Wang, X. Wu, X. Yuan, Z. Liu, Y. Zhang, L. Fu, Y. Zhu, Q. Zhou, Y. Wu, W. Huang, *Chem. Soc. Rev.* 46 (2017) 6816–6854.
- [11] J.T. Zhang, X.S. Zhao, *ChemSusChem* 5 (2012) 818–841.
- [12] P.J. Hall, M. Mirzaei, S.I. Fletcher, F.B. Sillars, A.J.R. Rennie, G.O. Shitta-Bey, G. Wilson, A. Cruden, R. Carter, *Energy Environ. Sci.* 3 (2010) 1238–1251.
- [13] K. Naoi, S. Ishimoto, J.-I. Miyamoto, W. Naoi, *Energy Environ. Sci.* 5 (2012) 9363.
- [14] J.H. Chae, X. Zhou, G.Z. Chen, *Green* 2 (2012) 41–54.
- [15] W. Zuo, R. Li, C. Zhou, Y. Li, J. Xia, J. Liu, *Adv. Sci.* 4 (2017) 1600539.
- [16] Z.P. Cano, D. Banham, S. Ye, A. Hintennach, J. Lu, M. Fowler, Z. Chen, *Nat. Energy* 3 (2018) 279–289.
- [17] Z. Yang, J. Ren, Z. Zhang, X. Chen, G. Guan, L. Qiu, Y. Zhang, H. Peng, *Chem. Rev.* 115 (2015) 5159–5223.
- [18] X. Zhang, H.T. Zhang, C. Li, K. Wang, X.Z. Sun, Y.W. Ma, *RSC Adv.* 4 (2014) 45862–45884.
- [19] Q. Gao, *J. Energy Chem.* 38 (2019) 219–224.
- [20] M. Sevilla, R. Mokaya, *Energy Environ. Sci.* 7 (2014) 1250–1280.
- [21] E. Frackowiak, Q. Abbas, F. Beguin, *J. Energy Chem.* 22 (2013) 226–240.
- [22] Z. Liu, H. Song, Y. Zhao, R. He, J. Meng, Q. Yu, K.A. Owusu, C. Yu, D. Zhao, L. Zhou, L. Mai, *ACS Mater. Lett.* 1 (2019) 290–296.
- [23] J. Ren, Y. Huang, H. Zhu, B. Zhang, H. Zhu, S. Shen, G. Tan, F. Wu, H. He, S. Lan, X. Xia, Q. Liu, *Carbon Energy* (2020) 1–27.
- [24] Y. Tang, Y. Zhang, W. Li, B. Ma, X. Chen, *Chem. Soc. Rev.* 44 (2015) 5926–5940.
- [25] Y. Xie, M. Saubanere, M.L. Doublet, *Energy Environ. Sci.* 10 (2017) 266–274.
- [26] Z. Lin, E. Goikolea, A. Balducci, K. Naoi, P.L. Taberna, M. Salanne, G. Yushin, P. Simon, *Mater. Today* 21 (2018) 419–436.
- [27] D. Bin, Y.P. Wen, Y.G. Wang, Y.Y. Xia, *J. Energy Chem.* 27 (2018) 1521–1535.
- [28] X.L. Wu, T. Wen, H.L. Guo, S. Yang, X. Wang, A.W. Xu, *ACS Nano* 7 (2013) 3589–3597.
- [29] J. Zhong, Z. Yang, R. Mukherjee, A. Varghese Thomas, K. Zhu, P. Sun, J. Lian, H. Zhu, N. Koratkar, *Nano Energy* 2 (2013) 1025–1030.
- [30] Q. Zhang, Z. Liu, B. Zhao, Y. Cheng, L. Zhang, H.-H. Wu, M.-S. Wang, S. Dai, K. Zhang, D. Ding, Y. Wu, M. Liu, *Energy Storage Mater.* 16 (2019) 632–645.
- [31] P.K. Adusei, S. Gbordzoe, S.N. Kanakaraj, Y.-Y. Hsieh, N.T. Alvarez, Y. Fang, K. Johnson, C. McConnell, V. Shanov, *J. Energy Chem.* 40 (2020) 120–131.
- [32] S. Feng, Z. Liu, Q. Yu, Z. Zhuang, Q. Chen, S. Fu, L. Zhou, L. Mai, *ACS Appl. Mater. Interfaces* 11 (2019) 4011–4016.
- [33] Z. Li, Z. Liu, H. Sun, C. Gao, *Chem. Rev.* 115 (2015) 7046–7117.
- [34] J. Yang, Z. Ju, Y. Jiang, Z. Xing, B. Xi, J. Feng, S. Xiong, *Adv. Mater.* 30 (2018) 1700104.
- [35] Y. Liu, H. Dai, L. Wu, W. Zhou, L. He, W. Wang, W. Yan, Q. Huang, L. Fu, Y. Wu, *Adv. Energy Mater.* 9 (2019) 1901379.
- [36] R. Väli, A. Jänes, T. Thomborg, E. Lust, *Electrochim. Acta* 253 (2017) 536–544.
- [37] Y.B. An, S. Chen, M.M. Zou, L.B. Geng, X.Z. Sun, X. Zhang, K. Wang, Y.W. Ma, *Rare Metals* 38 (2019) 1113–1123.
- [38] V. Presser, M. Heon, Y. Gogotsi, *Adv. Func. Mater.* 21 (2011) 810–833.
- [39] T. Morishita, T. Tsumura, M. Toyoda, J. Przepiórski, A.W. Morawski, H. Konno, M. Inagaki, *Carbon* 48 (2010) 2690–2707.
- [40] Y.H. Feng, S.H. Chen, J. Wang, B.A. Lu, *J. Energy Chem.* 43 (2020) 129–138.
- [41] M.J. Allen, V.C. Tung, R.B. Kaner, *Chem. Rev.* 110 (2010) 132–145.
- [42] L. Weinstein, R. Dash, *Mater. Today* 16 (2013) 356–357.
- [43] N. von der Assen, P. Voll, M. Peters, A. Bardow, *Chem. Soc. Rev.* 43 (2014) 7982–7994.
- [44] C. Costentin, M. Robert, J.M. Saveant, *Chem. Soc. Rev.* 42 (2013) 2423–2436.
- [45] J. Qiao, Y. Liu, F. Hong, J. Zhang, *Chem. Soc. Rev.* 43 (2014) 631–675.
- [46] J.C. Abanades, E.S. Rubin, M. Mazzotti, H.J. Herzog, *Energy Environ. Sci.* 10 (2017) 2491–2499.
- [47] J. Wei, Q. Ge, R. Yao, Z. Wen, C. Fang, L. Guo, H. Xu, J. Sun, *Nat. Commun.* 8 (2017) 15174.
- [48] S. Chu, Y. Cui, N. Liu, *Nat. Mater.* 16 (2016) 16–22.
- [49] J. Kothandaraman, A. Goepfert, M. Czaun, G.A. Olah, G.K. Prakash, *J. Am. Chem. Soc.* 138 (2016) 778–781.
- [50] M. Marszewski, S. Cao, J. Yu, M. Jaroniec, *Mater. Horiz.* 2 (2015) 261–278.
- [51] J. Wu, S. Ma, J. Sun, J.I. Gold, C. Tiwary, B. Kim, L. Zhu, N. Chopra, I.N. Odeh, R. Vajtai, A.Z. Yu, R. Luo, J. Lou, G. Ding, P.J. Kenis, P.M. Ajayan, *Nat. Commun.* 7 (2016) 13869.
- [52] E.V. Kondratenko, G. Mul, J. Baltrusaitis, G.O. Larrazabal, J. Perez-Ramirez, *Energy Environ. Sci.* 6 (2013) 3112–3135.
- [53] Y. Tamaura, M. Tahata, *Nature* 346 (1990) 255–256.

- [54] M. Motiei, Y. Rosenfeld Hacohen, J. Calderon-Moreno, A. Gedanken, J. Am. Chem. Soc. 123 (2001) 8624–8625.
- [55] Z. Lou, Q. Chen, Y. Zhang, W. Wang, Y. Qian, J. Am. Chem. Soc. 125 (2003) 9302–9303.
- [56] A. Chakrabarti, J. Lu, J.C. Skrabutenas, T. Xu, Z.L. Xiao, J.A. Maguire, N.S. Hosmane, J. Mater. Chem. 21 (2011) 9491–9493.
- [57] J. Zhang, Y. Zhao, X. Guan, R.E. Stark, D.L. Akins, J.W. Lee, J. Phys. Chem. C 116 (2012) 2639–2644.
- [58] R. He, Z. Wang, X. Jin, Carbon 116 (2017) 246–254.
- [59] S. Licht, A. Douglas, J. Ren, R. Carter, M. Lefler, C.L. Pint, ACS Cent. Sci. 2 (2016) 162–168.
- [60] W. Chu, M.F. Ran, X. Zhang, N. Wang, Y.F. Wang, H.P. Xie, X.S. Zhao, J. Energy Chem. 22 (2013) 136–144.
- [61] S. Baik, J.H. Park, J.W. Lee, Electrochim. Acta 330 (2020) 135264.
- [62] Y.K. Kim, J.H. Park, J.W. Lee, Carbon 126 (2018) 215–224.
- [63] H. Helmholtz, Ann. Phys. Chem. 89 (1853) 211–233.
- [64] X.L. Chen, R. Paul, L.M. Dai, National Sci. Rev. 4 (2017) 453–489.
- [65] F. Béguin, V. Presser, A. Balducci, E. Frackowiak, Adv. Mater. 26 (2014) 2219–2251.
- [66] G. Gouy, J. Phys. Theor. Appl. 9 (1910) 457–468.
- [67] O. Stern, Z. Elektrochem. Angew. P. 30 (1924) 508.
- [68] C. Zhong, Y. Deng, W. Hu, J. Qiao, L. Zhang, J. Zhang, Chem. Soc. Rev. 44 (2015) 7484–7539.
- [69] M. Conte, Fuel Cells 10 (2010) 806–818.
- [70] E. Frackowiak, F. Béguin, Carbon 39 (2001) 937–950.
- [71] P.L. Taberna, P. Simon, J.F. Fauvarque, J. Electrochem. Soc. 150 (2003) A292.
- [72] Y.Z. Wang, X.Y. Shan, D.W. Wang, H.M. Cheng, F. Li, J. Energy Chem. 38 (2019) 214–218.
- [73] L. Lv, Y. Fan, Q. Chen, Y. Zhao, Y. Hu, Z. Zhang, N. Chen, L. Qu, Nanotechnology 25 (2014) 235401.
- [74] Y. Meng, Y. Zhao, C. Hu, H. Cheng, Y. Hu, Z. Zhang, G. Shi, L. Qu, Adv. Mater. 25 (2013) 2326–2331.
- [75] D. Yu, K. Goh, H. Wang, L. Wei, W. Jiang, Q. Zhang, L. Dai, Y. Chen, Nat. Nanotechnol. 9 (2014) 555–562.
- [76] C. Li, X. Zhang, K. Wang, X. Sun, Y. Ma, J. Power Sources 400 (2018) 468–477.
- [77] X. Wang, Y. Zhang, C. Zhi, X. Wang, D. Tang, Y. Xu, Q. Weng, X. Jiang, M. Mitome, D. Golberg, Y. Bando, Nat. Commun. 4 (2013) 2905.
- [78] H. Bi, Z. Yin, X. Cao, X. Xie, C. Tan, X. Huang, B. Chen, F. Chen, Q. Yang, X. Bu, X. Lu, L. Sun, H. Zhang, Adv. Mater. 25 (2013) 5916–5921.
- [79] Y. Zhao, J. Liu, Y. Hu, H. Cheng, C. Hu, C. Jiang, L. Jiang, A. Cao, L. Qu, Adv. Mater. 25 (2013) 591–595.
- [80] M.F. El-Kady, Y.L. Shao, R.B. Kaner, Nat. Rev. Mater. 1 (2016) 16033.
- [81] Z. Zheng, P. Li, J. Huang, H. Liu, Y. Zao, Z. Hu, L. Zhang, H. Chen, M.-S. Wang, D.-L. Peng, Q. Zhang, J. Energy Chem. 41 (2020) 126–134.
- [82] Y.P. Zhai, Y.Q. Dou, D.Y. Zhao, P.F. Fulvio, R.T. Mayes, S. Dai, Adv. Mater. 23 (2011) 4828–4850.
- [83] X. Zhao, X. Zhang, C. Li, X. Sun, J. Liu, K. Wang, Y. Ma, A.C.S. Sustain. Chem. Eng. 7 (2019) 11275–11283.
- [84] B. Xu, S. Hou, H. Duan, G. Cao, M. Chu, Y. Yang, J. Power Sources 228 (2013) 193–197.
- [85] T. Kim, G. Jung, S. Yoo, K.S. Suh, R.S. Ruoff, ACS Nano 7 (2013) 6899–6905.
- [86] X.Y. Yang, L.H. Chen, Y. Li, J.C. Rooke, C. Sanchez, B.L. Su, Chem. Soc. Rev. 46 (2017) 481–558.
- [87] M. Inagaki, H. Konno, O. Tanaike, J. Power Sources 195 (2010) 7880–7903.
- [88] C. Li, X. Zhang, C.K. Sun, K. Wang, X.Z. Sun, Y.W. Ma, J. Phys. D Appl. Phys. 52 (2019) 143001.
- [89] B. Guo, Q. Liu, E. Chen, H. Zhu, L. Fang, J.R. Gong, Nano Lett. 10 (2010) 4975–4980.
- [90] Y. Chen, X. Qiu, L. Fan, J. Energy Chem. 48 (2020) 187–194.
- [91] K. Zhang, Z. Hu, J. Chen, J. Energy Chem. 22 (2013) 214–225.
- [92] X. Yu, C. Pei, L. Feng, Chinese Chem. Lett. 30 (2019) 1121–1125.
- [93] Y. Xu, Z. Lin, X. Zhong, X. Huang, N.O. Weiss, Y. Huang, X. Duan, Nat. Commun. 5 (2014) 4554.
- [94] T.H. Okabe, D.R. Sadoway, J. Mater. Res. 13 (1998) 3372–3377.
- [95] S. Choi, T. Bok, J. Ryu, J.-I. Lee, J. Cho, S. Park, Nano Energy 12 (2015) 161–168.
- [96] K.J. Lee, S. Choi, S. Park, H.R. Moon, Chem. Mater. 28 (2016) 4403–4408.
- [97] N. Lin, T. Li, Y. Han, Q. Zhang, T. Xu, Y. Qian, ACS Appl. Mater. Inter. 10 (2018) 8399–8404.
- [98] Z. Bao, M.R. Weatherspoon, S. Shian, Y. Cai, P.D. Graham, S.M. Allan, G. Ahmad, M.B. Dickerson, B.C. Church, Z. Kang, H.W. Abernathy Iii, C.J. Summers, M. Liu, K.H. Sandhage, Nature 446 (2007) 172–175.
- [99] W. Luo, B. Wang, X. Wang, W.F. Stickle, X. Ji, Chem. Commun. 49 (2013) 10676–10678.
- [100] B.V. Shafirovich, U.I. Goldshleger, Combust. Sci. Technol. 84 (1992) 33–43.
- [101] E.Y. Cunniff, D.S. Pyle, C.R. Merritt, C.L. Brown, C.J. Webb, E.M.A. Gray, Inter. J. Hydrogen Energy 39 (2014) 6783–6788.
- [102] D. Chen, H. Feng, J. Li, Chem. Rev. 112 (2012) 6027–6053.
- [103] H.L. Poh, Z. Sofer, J. Luxa, M. Puma, Small 10 (2014) 1529–1535.
- [104] J. Han, L.L. Zhang, S. Lee, J. Oh, K.S. Lee, J.R. Potts, J.Y. Ji, X. Zhao, R.S. Ruoff, S. Park, ACS Nano 7 (2013) 19–26.
- [105] P.P. Yu, Z.M. Zhang, L.X. Zheng, F. Teng, L.F. Hu, X.S. Fang, Adv. Energy Mater. 6 (2016) 1601111.
- [106] X. Sun, P. Cheng, H. Wang, H. Xu, L. Dang, Z. Liu, Z. Lei, Carbon 92 (2015) 1–10.
- [107] X. Yu, S.K. Park, S.-H. Yeon, H.S. Park, J. Power Sources 278 (2015) 484–489.
- [108] X. Wang, G. Sun, P. Routh, D.H. Kim, W. Huang, P. Chen, Chem. Soc. Rev. 43 (2014) 7067–7098.
- [109] C.N.R. Rao, K. Gopalakrishnan, A. Govindaraj, Nano Today 9 (2014) 324–343.
- [110] Z.S. Wu, A. Winter, L. Chen, Y. Sun, A. Turchanin, X. Feng, K. Mullen, Adv. Mater. 24 (2012) 5130–5135.
- [111] H. Zhang, X. Zhang, X. Sun, D. Zhang, H. Lin, C. Wang, H. Wang, Y. Ma, ChemSusChem 6 (2013) 1084–1090.
- [112] Z. Wen, X. Wang, S. Mao, Z. Bo, H. Kim, S. Cui, G. Lu, X. Feng, J. Chen, Adv. Mater. 24 (2012) 5610–5616.
- [113] Y. Wu, X. Liu, D. Xia, Q. Sun, D. Yu, S. Sun, X. Liu, Y. Teng, W. Zhang, X. Zhao, Chinese Chem. Lett. 31 (2020) 559–564.
- [114] Q. Yu, J. Lv, Z. Liu, M. Xu, W. Yang, K.A. Owusu, L. Mai, D. Zhao, L. Zhou, Sci. Bull. 64 (2019) 1617–1624.
- [115] J. Zhang, T. Tian, Y.H. Chen, Y.F. Niu, J. Tang, L.C. Qin, Chem. Phys. Lett. 591 (2014) 78–81.
- [116] R. Raccichini, A. Varzi, S. Passerini, B. Scrosati, Nat. Mater. 14 (2015) 271–279.
- [117] H. Zhang, X. Zhang, X. Sun, Y. Ma, Sci. Rep. 3 (2013) 3534.
- [118] H.T. Zhang, X.Z. Sun, X. Zhang, H. Lin, K. Wang, Y.W. Ma, J. Alloy Compd. 622 (2015) 783–788.
- [119] Z.Y. Xing, B. Wang, W.Y. Gao, C.Q. Pan, J.K. Halsted, E.S. Chong, J. Lu, X.F. Wang, W. Luo, C.H. Chang, Y.H. Wen, S.Q. Ma, K. Amine, X.L. Ji, Nano Energy 11 (2015) 600–610.
- [120] M.F. De Volder, S.H. Tawfik, R.H. Baughman, A.J. Hart, Science 339 (2013) 535–539.
- [121] C.-M. Seah, S.-P. Chai, A.R. Mohamed, Carbon 70 (2014) 1–21.
- [122] C.L. Wang, F.T. Li, H.L. Qu, Y.A. Wang, X.L. Yi, Y. Qiu, Z.J. Zou, Y.S. Luo, B.H. Yu, Electrochim. Acta 158 (2015) 35–41.
- [123] Z. Lou, Q. Chen, W. Wang, Y. Zhang, Carbon 41 (2003) 3063–3067.
- [124] L. Chang, W. Wei, K. Sun, Y.H. Hu, J. Mater. Chem. A 3 (2015) 10183–10187.
- [125] W. Wei, K. Sun, Y.H. Hu, J. Mater. Chem. A 2 (2014) 16842–16846.
- [126] J. Hu, Z. Guo, W. Chu, L. Li, T. Lin, J. Energy Chem. 24 (2015) 620–625.
- [127] J.S. Zhang, J.W. Lee, Carbon 53 (2013) 216–221.
- [128] J.S. Zhang, J.W. Lee, A.C.S. Sustain. Chem. Eng. 2 (2014) 735–740.
- [129] W. Lee, G.M. Kim, S. Baik, J.W. Lee, Electrochim. Acta 210 (2016) 743–753.
- [130] H. Tang, P. Gao, X. Liu, H. Zhu, Z. Bao, J. Mater. Chem. A 2 (2014) 15734–15739.
- [131] H. Huang, C. Cheng, S. Liang, C. Liang, Y. Xia, Y. Gan, J. Zhang, X. Tao, W. Zhang, Carbon 130 (2018) 559–565.
- [132] C. Liang, L. Pan, S. Liang, Y. Xia, Z. Liang, Y. Gan, H. Huang, J. Zhang, W. Zhang, Small 15 (2019) 1902249.
- [133] J. Wang, R. Ma, Z. Zhou, G. Liu, Q. Liu, Sci. Rep. 5 (2015) 9304.
- [134] Z.H. Sheng, L. Shao, J.J. Chen, W.J. Bao, F.B. Wang, X.H. Xia, ACS Nano 5 (2011) 4350–4358.
- [135] H. Yin, P. Chen, C. Xu, X. Gao, Q. Zhou, Y. Zhao, L. Qu, Carbon 94 (2015) 928–935.
- [136] A.G. Merzhanov, J. Mater. Chem. 14 (2004) 1779.
- [137] G. Liu, K. Chen, H. Zhou, J. Guo, K. Ren, J.M.F. Ferreira, Mater. Lett. 61 (2007) 779–784.
- [138] S.B. Jin, P. Shen, D.S. Zhou, Q.C. Jiang, Cryst. Growth Design 12 (2012) 2814–2824.
- [139] B.Y. Li, L.J. Rong, Y.Y. Li, V.E. Gjunter, Acta Mater. 48 (2000) 3895–3904.
- [140] X. Su, F. Yu, Y. Yan, G. Zheng, T. Liang, Q. Zhang, X. Cheng, D. Yang, H. Chi, X. Tang, Q. Zhang, C. Uher, Nat. Commun. 5 (2014) 4908.
- [141] Y. Li, G. Liu, T. Cao, L. Liu, J. Li, K. Chen, L. Li, Y. Han, M. Zhou, Adv. Funct. Mater. 26 (2016) 6025–6032.
- [142] C. Li, X. Zhang, K. Wang, X. Sun, G. Liu, J. Li, H. Tian, J. Li, Y. Ma, Adv. Mater. 29 (2017) 1604690.
- [143] N. Lu, G. He, J. Liu, G. Liu, J. Li, Ceram. Inter. 44 (2018) 2463–2469.
- [144] C. Li, X. Zhang, K. Wang, X. Sun, Y. Ma, J. Power Sources 414 (2019) 293–301.
- [145] J. Lang, X. Zhang, B. Liu, R. Wang, J. Chen, X. Yan, J. Energy Chem. 27 (2018) 43–56.
- [146] X.Y. Shan, Y.Z. Wang, D.W. Wang, F. Li, H.M. Cheng, Adv. Energy Mater. 6 (2016) 1502064.
- [147] C. Zhan, X. Zeng, X. Ren, Y. Shen, R. Lv, F. Kang, Z.-H. Huang, J. Energy Chem. 42 (2020) 180–184.
- [148] S. Zhang, C. Li, X. Zhang, X. Sun, K. Wang, Y. Ma, ACS Appl. Mater. Interfaces 9 (2017) 17136–17144.
- [149] J. Li, Z. Liu, Q. Zhang, Y. Cheng, B. Zhao, S. Dai, H.-H. Wu, K. Zhang, D. Ding, Y. Wu, M. Liu, M.-S. Wang, Nano Energy 57 (2019) 22–33.
- [150] C. Li, X. Zhang, K. Wang, X. Sun, Y. Ma, Carbon 140 (2018) 237–248.
- [151] P. Simon, Y. Gogotsi, Acc. Chem. Res. 46 (2013) 1094–1103.
- [152] J. Wang, S. Kaskel, J. Mater. Chem. 22 (2012) 23710.
- [153] D.S. Su, G. Centi, J. Energy Chem. 22 (2013) 151–173.
- [154] K. Gopalsamy, Q. Yang, S. Cai, T. Huang, Z. Gao, C. Gao, J. Energy Chem. 34 (2019) 104–110.
- [155] N. Liu, Z. Pan, X. Ding, J. Yang, G. Xu, L. Li, Q. Wang, M. Liu, Y. Zhang, J. Energy Chem. 41 (2020) 209–215.
- [156] H. Li, Y. Tao, X. Zheng, J. Luo, F. Kang, H.-M. Cheng, Q.-H. Yang, Energy Environ. Sci. (2016).